Article

Autoimmune response to C9orf72 protein in amyotrophic lateral sclerosis

https://doi.org/10.1038/s41586-025-09588-6

Received: 4 February 2025

Accepted: 2 September 2025

Published online: 01 October 2025

Open access

Check for updates

Tanner Michaelis[1], Cecilia S. Lindestam Arlehamn[1,2,17], Emil Johansson[1,3,17], April Frazier[1], James D. Berry[4,5], Merit Cudkowicz[4,5], Namita A. Goyal[6], Christina Fournier[7], Allison Snyder[8], Justin Y. Kwan[9], Jody Crook[9], Elizabeth J. Phillips[10,11], Simon A. Mallal[10,11], John Ravits[12], Karen S. Marder[13], John Sidney[1], David Sulzer[14,15] ✉ & Alessandro Sette[1,16] ✉

Amyotrophic lateral sclerosis (ALS) is a neurodegenerative disease characterized by a progressive loss of motor neurons. Neuroinflammation is apparent in affected tissues, including increased T cell infiltration and activation of microglia, particularly in the spinal cord[1,2]. Autoimmune responses are thought to have a key role in ALS pathology, and it is hypothesized that T cells contribute to the rapid loss of neurons during disease progression[3,4]. However, until now there has been no reported target for such an autoimmune response. Here we show that ALS is associated with recognition of the C9orf72 antigen, and we map the specific epitopes that are recognized. We show that these responses are mediated by $CD4^+$ T cells that preferentially release IL-5 and IL-10, and that IL-10-mediated T cell responses are significantly greater in donors who have a longer predicted survival time. Our results reinforce the previous hypothesis that neuroinflammation has an important role in ALS disease progression, possibly because of a disrupted balance of inflammatory and counter-inflammatory T cell responses[4]. These findings highlight the potential of therapeutic strategies aimed at enhancing regulatory T cells[5], and identify a key target for antigen-specific T cell responses that could enable precision therapeutics in ALS.

ALS is a neurodegenerative disease with a mean life expectancy of around four years after diagnosis. It is characterized by extensive damage to oligodendrocytes and a loss of motor neurons, leading to paralysis. Neuroinflammation is apparent in the affected tissues, and includes high levels of T cell infiltration—mainly by $CD8^+$ cytotoxic cells but also by $CD4^+$ T helper cells—and increased expression of human leukocyte antigen (HLA) class I and II molecules by microglia, particularly in the spinal cord[1,2]. It has long been hypothesized that an autoimmune process, including specific T cells, mediates the rapid loss of neurons during the disease[3,4], but no direct evidence has been reported for such a response.

A hallmark of ALS, like many neurodegenerative disorders, is the cytoplasmic inclusion of proteins such as TAR-DNA binding protein (TDP-43), particularly in oligodendrocytes and motor neurons[6]. In Parkinson's disease (PD) and related Parkinsonian disorders, alpha-synuclein (α-syn), the main component of Lewy body inclusions, has been found to be a target of autoreactive T cells[7]. However, two previous studies have been unable to identify a similar response to TDP-43 in individuals with ALS[8,9]. A differential T cell response was also not found for senataxin, a protein that is associated with a juvenile form of ALS (ALS4)[8]. In summary, previous studies have not identified a trigger for autoimmune responses in ALS.

More than 25 genetic mutations have been associated with ALS, including mutant alleles of TDP-43 and of superoxide dismutase 1 (SOD1). The most common mutation affects the gene encoding the protein C9orf72. Mutations in C9orf72 are present in 40% of familial ALS cases and around 10% of sporadic ALS cases, and are also associated with frontotemporal dementia[10,11]. The disease-associated mutations of C9orf72 produce an expansion of a hexanucleotide repeat in a nominally non-coding region, although these repeats are thought to encode smaller peptides composed of dipeptide repeats that might affect proteolytic processing[12]. Expansions of nucleotide repeats are also found in genes associated with other developmental and degenerative disorders, including Huntington's disease, Fragile X syndrome, spinocerebellar ataxias and Friedreich's ataxia. It is widely thought that ALS is associated with decreased expression of C9orf72, and that loss

[1]Center for Autoimmunity and Inflammation, La Jolla Institute for Immunology, La Jolla, CA, USA. [2]Center for Vaccine Research, Department of Infectious Disease Immunology, Statens Serum Institut, Copenhagen, Denmark. [3]Department of Experimental Medical Science, Wallenberg Neuroscience Center and Lund Stem Cell Center, Lund University, Lund, Sweden. [4]Sean M. Healey and AMG Center for ALS, Department of Neurology, Massachusetts General Hospital, Harvard Medical School, Boston, MA, USA. [5]Department of Neurology, Massachusetts General Hospital, Harvard Medical School, Boston, MA, USA. [6]Department of Neurology, University of California, Irvine, Irvine, CA, USA. [7]Department of Neurology, Emory University, Atlanta, GA, USA. [8]Penn Frontotemporal Degeneration Center, Department of Neurology, Perelman School of Medicine, University of Pennsylvania, Philadelphia, PA, USA. [9]National Institute of Neurological Disorders and Stroke, National Institutes of Health, Bethesda, MD, USA. [10]Institute for Immunology and Infectious Diseases, Murdoch University, Perth, Western Australia, Australia. [11]Vanderbilt University School of Medicine, Nashville, TN, USA. [12]Department of Neurosciences, School of Medicine, University of California, San Diego, La Jolla, CA, USA. [13]Department of Neurology, Columbia University Irving Medical Center, New York, NY, USA. [14]Division of Molecular Therapeutics, New York State Psychiatric Institute, New York, NY, USA. [15]Departments of Psychiatry, Neurology and Pharmacology, Columbia University, New York, NY, USA. [16]Department of Medicine, Division of Infectious Diseases and Global Public Health, University of California, San Diego, La Jolla, CA, USA. [17]These authors contributed equally: Cecilia S. Lindestam Arlehamn, Emil Johansson. ✉e-mail: ds43@cumc.columbia.edu; alex@lji.org

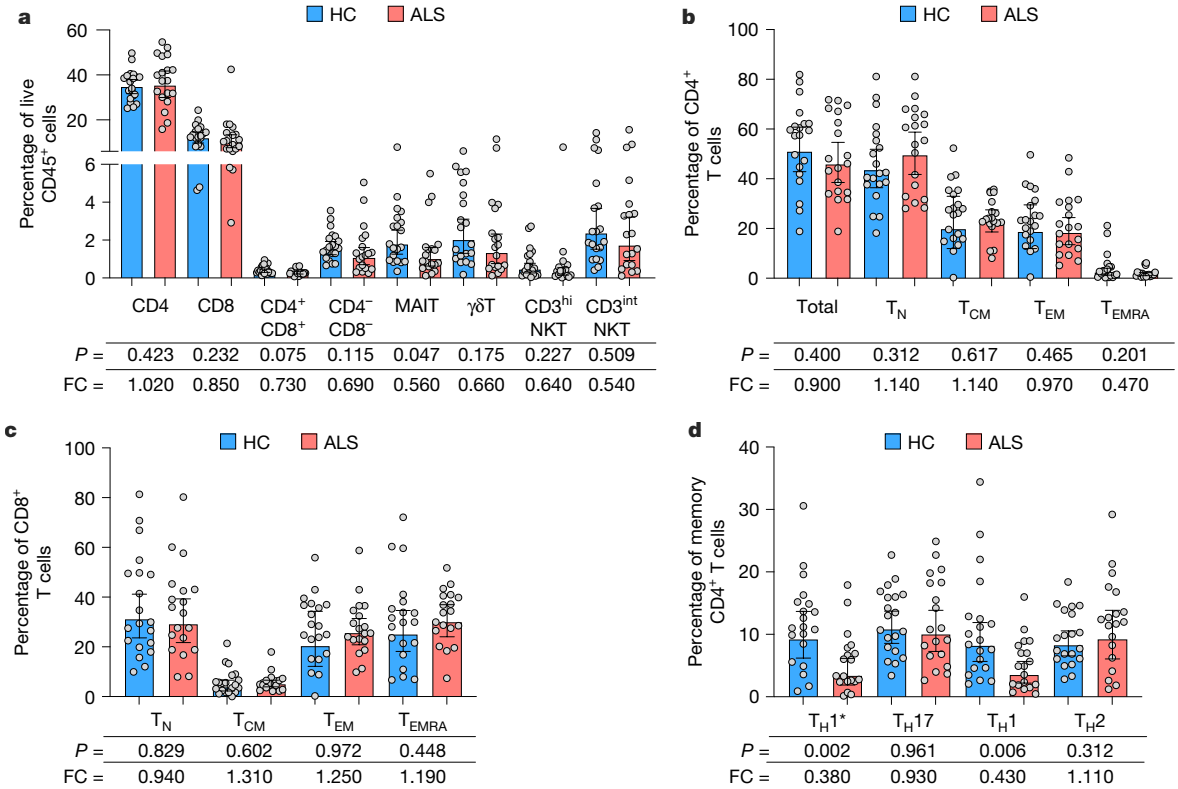

Fig. 1 | Immunophenotyping shows alterations in the T helper cell subsets associated with ALS. a–**c**, Broad representation of lymphocyte subsets (**a**) and CD4 (**b**) or CD8 (**c**) memory T cell subsets in individuals with ALS ($n = 19$) and in healthy control (HC) donors ($n = 20$). NKT, natural killer T cell. **d**, Composition of functional T helper cell subsets defined on the basis of expression of the CCR6, CXCR3 and CCR4 subset markers, in the same donors as in **a**–**c**. *P* values from two-tailed Mann–Whitney tests and geometric mean ± 95% confidence intervals are shown. Fold change (FC) values represent the ratio of geometric values in the ALS–HC cohorts.

of C9orf72 function contributes to disease pathogenesis[13], suggesting that an autoimmune attack on C9orf72 might result in decreased expression and influence pathogenesis.

Here we report an association of ALS with recognition of the C9orf72 antigen, and map the specific epitopes that are recognized. These responses are mediated by $CD4^+$ T cells that preferentially release IL-5 and IL-10. We found that the frequency of IL-10-releasing C9orf72-specific T cells was significantly higher in donors with ALS who had a longer predicted survival time, raising the possibility that the T cells might have a regulatory and protective influence on disease progression.

Donor characteristics

We analysed peripheral blood mononuclear cells (PBMCs) from whole-blood donations from 40 individuals with ALS and 28 age- and sex-matched healthy controls. Study participants were recruited from four collaborating clinic sites across the USA: Emory University (Atlanta, Georgia); the National Institute for Neurological Disorders and Stroke at the National Institutes of Health (Bethesda, Maryland); the University of California, Irvine (Irvine, California); and Harvard Medical School/Massachusetts General Hospital (Boston, Massachusetts). In addition, nine of the study participants with ALS were recruited through Sanguine Biosciences (Woburn, Massachusetts), a contract research organization.

Demographics and clinical characteristics of the cohort are shown in Extended Data Table 1. The male:female distribution was 24:16 for individuals with ALS, and 19:9 for age-matched healthy controls. The higher male representation in the ALS cohort is representative of the higher disease incidence in male individuals[14] and participants at the specific clinical sites participating in the study. The cohort was age-matched (control, median 59.0, range 29–82; ALS, median 61.0, range 45–81; $P = 0.680$ by two-tailed Mann–Whitney test, which was used here and throughout the rest of the manuscript). The median time of blood donation after symptom onset was 36 months (24.0 for male individuals and 48.0 for female individuals; $P = 0.023$). The median time after ALS diagnosis was 12.0 months (12.0 for male individuals and 18.0 for females individuals; $P = 0.599$). The revised ALS functional rating scale (ALSFRS-R) score—a measure of disease severity in ALS that captures aspects of bodily function including speech, handwriting, walking and breathing—was recorded at the time of diagnosis and at follow-up to measure disease progression. ALSFRS-R scores were recorded at the time of blood donation; scores were 38.0 (median) for donors with ALS ($n = 33$) (39.0 for male individuals and 37.0 for female individuals; $P = 0.329$).

T helper cell subsets are altered in ALS

Conflicting reports have been published on variations in lymphocyte subsets in association with ALS[15]. Using flow cytometry, we determined the frequencies of different cell subsets in the ALS and control cohorts[16] (Extended Data Fig. 1), and identified a reduction in the frequency of mucosal-associated invariant T (MAIT) cells ($P = 0.047$; Fig. 1a), defined by the co-expression of CD3, CD161 and CD26. The comparisons of these cell subsets were not corrected for multiple testing because they are independent of each other, but the statistical significance in MAIT frequency would be likely to be lost if correction for multiple testing were to be applied. We found no further significant differences in the major T cell subsets (Fig. 1a) or in the $CD4^+$ and $CD8^+$ memory T cell subsets (Fig. 1b,c), defined on the basis of CD45RA and CCR7 expression as naive T cells (T_N; $CD45RA^+CCR7^+$), central memory T cells (T_{CM}; $CD45RA^-CCR7^+$), effector memory T cells (T_{EM}; $CD45RA^-CCR7^-$) and

effector memory T cells expressing CD45RA (T_{EMRA}; $CD45RA^+CCR7^-$). However, within the functional $CD4^+$ T helper cell subset, defined by the expression of CCR6, CXCR3 and CCR4 subset markers[17], we found significant decreases in the frequency of T_H1^* cells—a subset of T helper cells with a phenotype similar to that of both T_H17 and T_H1 cells[16]—and in the frequency of T_H1 cell subsets, in individuals with ALS compared with healthy control donors ($P = 0.002$ and $P = 0.006$, respectively; Fig. 1d).

Autoantigenic T cell responses in ALS

We then investigated whether there were autoimmune responses against possible antigens associated with ALS, including TDP-43, SOD1 and C9orf72, following an approach that was previously used to define autoreactive epitope sequences from individuals with PD[7,18]. Accordingly, we synthesized complete sets of 15-amino-acid peptides overlapping by 10 residues spanning the entire sequence of each of these proteins[19].

Owing to the low frequency of autoreactive T cells[7,18,20], PBMCs were stimulated with the peptide sets to expand autoantigen-specific T cells, to obtain sufficient cells for reliable phenotyping of the T cell responses. After two weeks of in vitro expansion, FluoroSpot assays were used to measure T cell responses to the peptide pools by measuring the release of interferon-γ (IFNγ), a classical response by pro-inflammatory T_H1 and T_H1^* $CD4^+$ T cells, and interleukin-5 (IL-5) and IL-10, which are associated with T_H2 and/or regulatory $CD4^+$ cells. In addition to the TDP-43, SOD1 and C9orf72 pools, we included a positive control pool for T cell reactivity, encompassing epitopes derived from Epstein–Barr virus (EBV), for which nearly 100% of the US population is seropositive[21,22], and which has been used extensively as a positive control owing to the high-magnitude T cell response detected in most individuals[19].

Overall antigenic responses, defined as the total sum of IFNγ, IL-5 and IL-10 responses detected against each pool, are presented in Fig. 2a. Notably, a significant and selective increase in overall responses to the C9orf72 peptide pool was observed in participants with ALS, with the geometric mean responses approximately 4.15-fold higher in the ALS group compared with the controls ($P = 0.001$). In comparison, no significant difference was noted in the case of the TDP-43 or SOD1 pools, or the EBV control pool. These data suggest that C9orf72 is preferentially targeted by autoreactive T cells in the context of ALS.

Profiling of C9orf72-specific responses

We then examined the C9orf72 responses in terms of the relative balance of production of cytokines to determine which cytokines account for the differential responses of participants with ALS and healthy controls. All three cytokines were detected in ALS and control cohorts (Fig. 2b–d), and the differences were most prominent for IL-5 production (fold change = 5.13; $P = 0.002$). Differences in the production of IL-10 (fold change = 3.08; $P = 0.004$) and IFNγ (fold change = 2.08; $P = 0.037$) were smaller but still significant. These comparisons were not adjusted for multiple comparisons, because they are independent of each other. Because the difference in IFNγ-mediated T cell responses was close to the limit of significance, statistical significance would be likely to be lost if correction for multiple comparisons were to be applied.

In individuals with ALS, IFNγ accounted for 31.7% of the responses towards C9orf72, IL-5 for 45.6% and IL-10 for 22.8%; in healthy controls, the percentages were 54.9%, 27.0% and 19.0% for IFNγ, IL-5, and IL-10, respectively (Fig. 2e). Thus, although autoimmune T cell responses were of higher magnitude in people with ALS, the proportion of the autoreactive T cells that released IL-5 was higher in individuals with ALS than it was in healthy controls ($P = 0.014$), and, by contrast, the proportion of IFNγ responses was higher in healthy controls than it was in those with ALS ($P = 0.007$; Extended Data Fig. 2a,b). In line with an IL-5 biased response, we found that the IFNγ/IL-5 ratio was significantly lower in individuals with ALS ($P = 0.047$; Extended Data Fig. 2c).

To further characterize the C9orf72-reactive T cells, we restimulated PBMCs with serial dilutions of the C9orf72 peptide pool to compare the functional avidity of the IFNγ-, IL-5- and IL-10-releasing T cells. Of note, we found that the IFNγ-releasing cells in individuals with ALS had an approximately twofold lower avidity compared with those of healthy controls ($P = 0.016$; Fig. 2f,g), whereas no difference was observed for IL-5- or IL-10-releasing cells. We conclude that ALS is associated with a skewing of autoreactive T cell responses towards the T_H2-like phenotype, consistent with the overall reduction in T_H1/T_H1^*-like subsets (Fig. 1d), and a concurrent reduction in the avidity of IFNγ-releasing cells in response to C9orf72 epitopes.

C9orf72-specific responses in PD and AD

To assess whether C9orf72-specific T cell responses are specific for ALS or represent a general feature of neurodegenerative disorders, we measured responses of T cells towards C9orf72 peptides in participants diagnosed with PD or Alzheimer's disease (AD)[23,24] (Extended Data Table 2). Notably, when comparing these individuals with the previously screened ALS and control cohorts, we found that participants with PD or AD had significantly increased total and IFNγ-mediated T cell responses towards C9orf72, compared with control individuals (Extended Data Fig. 2d–g). However, similar to the control group, their responses were found to be mediated mainly by IFNγ, and the proportion of the total response mediated by IFNγ and IL-5 differed significantly between individuals with ALS and those with PD or AD (Extended Data Fig. 2h–j).

Phenotyping of C9orf72-specific T cells

We next assessed the representation of $CD4^+$ versus $CD8^+$ T cell subsets in PBMC cell cultures after two weeks of restimulation with the C9orf72 peptide pool, using flow cytometry (Extended Data Fig. 3). In both ALS and control samples, analysis of live single $CD3^+$ cells revealed that $CD4^+$ T cells were predominant (control: $CD4^+$, 83.5% of live $CD3^+$ cells; $CD8^+$, 8.9%; $P < 0.001$ (Extended Data Fig. 4a); ALS: $CD4^+$, 91.9%; $CD8^+$, 4.8%, $P < 0.001$ (Extended Data Fig. 4b)).

To further characterize the phenotype of C9orf72-specific T cells, we performed intracellular cytokine staining (ICS) assays to quantify cells producing IFNγ, IL-4, IL-10 and IL-17 in response to antigen stimulation after the two-week culture period (Extended Data Fig. 3). IL-4 was chosen as a representative T_H2 cytokine because this cytokine is more readily detected by ICS than is IL-5. Cytokine-producing cells in both control and ALS cohorts were mostly associated with a $CD4^+$ phenotype (control: $CD4^+$, median 2.0; $CD8^+$, 0.25; $P < 0.001$ (Extended Data Fig. 4c); ALS: $CD4^+$, median 1.4; $CD8^+$, 0.07; $P = 0.003$ (Extended Data Fig. 4d)). Cytokine production by $CD4^+$ T cells from healthy controls was highest for IFNγ, and for individuals with ALS it was highest for the T_H2 cytokine IL-4 (Extended Data Fig. 4e,f), reflecting a trend for a reduced proportion of IFNγ responses in individuals with ALS compared with controls ($P = 0.078$; Extended Data Fig. 4g). Indeed, we found that the IFNγ/IL-4, IFNγ/IL-10 and IFNγ/IL-4 + IL-10 ratios were all significantly lower in individuals with ALS ($P = 0.032$, $P = 0.049$ and $P = 0.008$, respectively; Extended Data Fig. 4h–j), confirming a T cell response skewed away from IFNγ in ALS, as seen in Fig. 2.

In conclusion, C9orf72 responses were mediated mostly by $CD4^+$ T cells. These responses were associated with a relative bias in favour of IL-4 and IL-10 production in the case of ALS samples and an IFNγ bias in the case of control samples.

Identification of recognized C9orf72 epitopes

To identify the specific epitopes recognized within C9orf72, we assayed responses by 28 individuals with ALS. After two weeks of in vitro culture, responses were deconvoluted by assaying 'mesopools' consisting of pools of around ten individual peptides, which were then deconvoluted

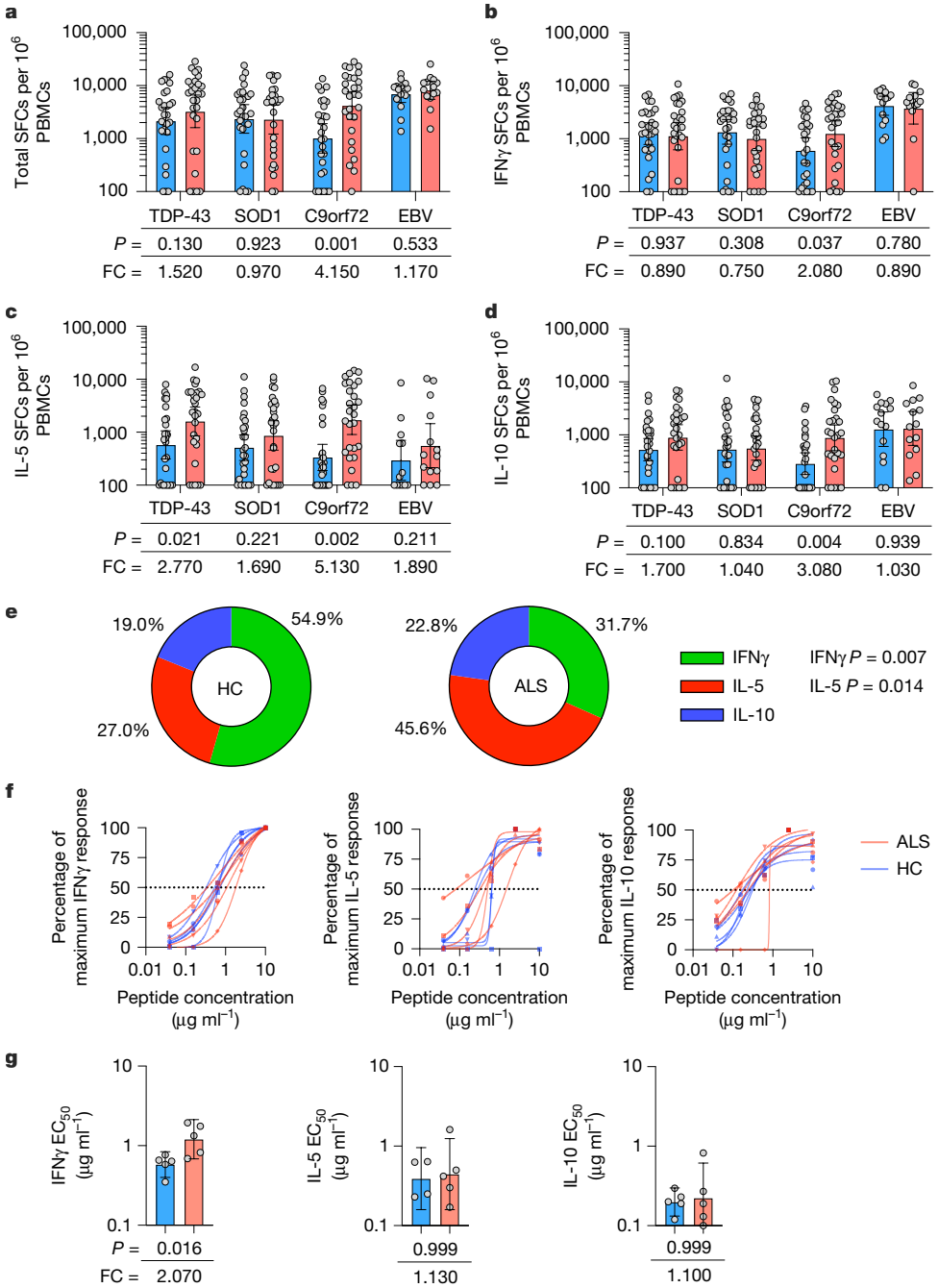

Fig. 2 | Cytokine responses towards neuroantigens in individuals with ALS and in healthy control individuals. a, Total IFNγ, IL-5 and IL-10 responses detected against each pool in HC donors ($n = 28$) and individuals with ALS ($n = 28$). **b**–**d**, Production of IFNγ (**b**), IL-5 (**c**) and IL-10 (**d**) individual cytokines, in the same donors as in **a**. SFCs, spot-forming cells. **e**, Relative balance of average IFNγ, IL-5 and IL-10 responses in HC individuals and in individuals with ALS. **f**, IFNγ-mediated (left), IL-5-mediated (middle) and IL-10-mediated (right) T cell responses towards serially diluted concentrations of the C9orf72 peptide pool in HC individuals ($n = 5$) and individuals with ALS ($n = 5$). **g**, Corresponding peptide concentration required to achieve 50% of the maximum response (EC_{50}) in HC donors ($n = 5$) and those with ALS ($n = 5$). For one HC donor, the lack of IL-5 responses prevented the development of a dose–response curve. *P* values from two-tailed Mann–Whitney tests and geometric mean ± 95% confidence intervals are shown. Fold change values represent the ratio of geometric values in the ALS–HC cohorts. HC donors are shown in blue; ALS donors in red.

to identify individual epitopes. In all 28 participants, individual epitopes were identified, as detailed in Supplementary Table 1. The epitopes spanned the entire C9orf72 sequence (Fig. 3a and Supplementary Table 1). High immunogenicity was associated with regions spanning residues 41–95, 266–295 and 361–445. Most ($n = 20$ of 28) individuals with ALS recognized multiple epitopes (median 3, range 0–26; Fig. 3b).

Twenty-three C9orf72-derived peptides were recognized by three or more individuals, highlighting the broad immunogenicity of the C9orf72 protein. The most frequently recognized epitopes are listed in Table 1, including sequences, position, overall response frequency and average response magnitude for responding individuals. The most frequently recognized epitope was 56-DGEITFLANHTLNGE-70, which was recognized in 32% of the individuals. Other frequently recognized epitopes were 366-IFQDVLHRDTLVKAF-380 (in 30%), 426-PFKSLRNLKIDLDLT-440 (in 26%), 431-RNLKIDLDLZAEGDL-445 (also in 26%) and 81-DVKFFVLSEKGVIIV-95 (in 23%) (Fig. 3a).

To identify potential HLA-restricted peptides, we next HLA-typed the participants with ALS included in the deconvolution experiment.

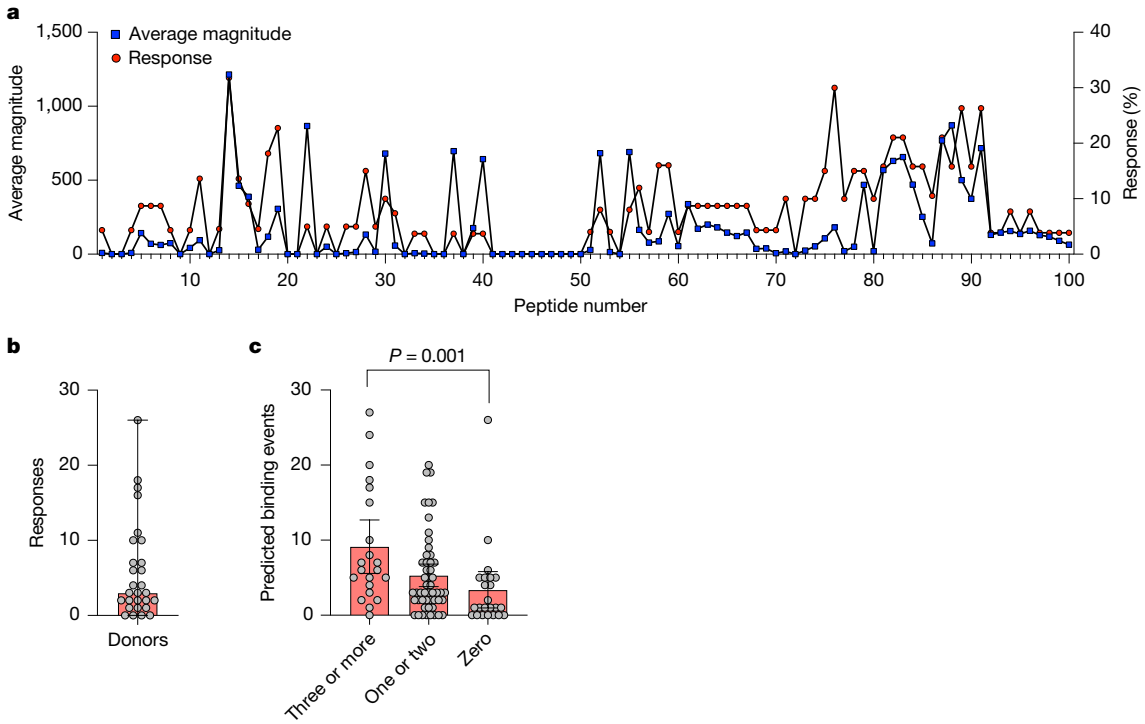

Fig. 3 | Mapping specific C9orf72 epitopes from responding individuals with ALS. a, Distribution of recognized epitopes among the 100 peptides spanning the C9orf72 protein sequence, identified in 28 participants with ALS. **b**, Number of epitopes recognized by each patient with ALS ($n = 28$) (median of 3, range 0–26). Median and range are shown. **c**, Number of predicted binding events to the 27 most common HLA II allelic variants, by peptides recognized in three or more patients ($n = 21$), one or two patients ($n = 51$) or no patients ($n = 23$). Binding was predicted using the NetMHCIIpan 4.1 EL prediction method, using a cut-off for a binding event as a predicted binding percentile score threshold of 20% or less[26]. *P* value from two-tailed Mann–Whitney test and mean ± 95% confidence intervals are shown.

Using the restrictor analysis tool for epitopes (RATE) algorithm[25], we identified 13 HLA–peptide combinations that were significantly associated with a detectable T cell response. Using the NetMHCIIpan-4.1 EL algorithm[26], we verified that significant peptide binding to the corresponding HLA molecule was predicted for seven of these interactions. Peptide 41-VRHIWAPKTEQVLLS- was restricted to DRB1*14:01; peptide 366-IFQDVLHRDTLVKAF-380 to DRB1*03:01; peptides 361-TPDLNIFQDVLHRDT-375 and 381-LDQVFQLKPGLSLRS-395 to DRB1*01:02; and the three peptides 406-HRKALTLIKYIEDDT-420, 426-PFKSLRNLKIDLDLT-440 and 431-RNLKIDLDLTAEGDL-445 to DQB1*05:01 (Table 2).

The C9orf72 protein can contain multiple phosphorylated residues. We compared the immunogenicity of phosphorylated or non-phosphorylated peptides at positions 1–15, 6–20, 426–440, 431–445 and 436–450. In general, similar reactivity was noted for the phosphorylated and non-phosphorylated peptides (Supplementary Table 1).

Binding capacity of C9orf72 peptides

We then assessed the predicted HLA binding of the C9orf72 antigenic peptides for a panel of the 27 most common HLA II allelic variants[27,28]. The 23 most dominant epitopes recognized in three or more participants with ALS were associated with predicted HLA class II binding to 9 ± 7.8 of the 27 HLA alleles. By contrast, epitopes recognized by only one or two patients were associated with binding to 5 ± 5.3 of the alleles, whereas peptides recognized by no one were associated with binding to 3 ± 5.6 predicted alleles (Fig. 3c). The number of predicted binding events was significantly higher for the peptides recognized in three or more patients than for the peptides recognized in no individuals ($P = 0.001$). Similarly, we observed a positive correlation between the response frequency and the number of the 27 HLA alleles predicted to bind to each peptide ($r = 0.339$, $P = 0.001$; Extended Data Fig. 5a). We further observed that the predicted binding strength, represented as a normalized rank value in which a small value indicates high affinity[25], was significantly lower for the 72 peptides recognized in one or more individuals, compared with the peptides not recognized in any individual ($P = 0.010$; Extended Data Fig. 5b). Overall, these results indicate that HLA binding influences C9orf72 epitope reactivity and that the most dominant epitopes are likely to be associated with presentation by multiple common HLA alleles; that is, exhibit a promiscuous HLA-binding capacity. We next investigated whether SOD1 and TDP-43 peptides were also predicted to bind HLA II. As shown in Extended Data Fig. 5c, TDP-43 and SOD1 peptides are predicted to bind the most common 27 HLA-DR, -DQ, and -DP HLA class II allelic variants, with no statistically significant difference ($P = 0.266$) in the number of HLA class II allelic variants predicted to bind to TDP-43 (median 2, range 0–22), SOD1 (median 1.5, range 0–23) or C9orf72 (median 1, range = 0–27)). Thus, the increased response to C9orf72 is not due to a lack of HLA class II binding for SOD1 and TDP-43. We hypothesize that the C9orf72 immunogenicity could be due to the decreased expression of C9orf72 in $CD14^+$ monocytes[13], leading to a loss of peripheral tolerance to C9orf72. No loss of expression of SOD1 or TDP-43 has been reported in peripheral cells, which could explain why the tolerance to these proteins has not been affected. Alternatively, this phenomenon could be related to an autophagy-related increase in the secretion of C9orf72[29,30]; because TDP-43 and SOD1 are not involved in autophagy, they might be absent or present at low levels in exosomes.

C9orf72 responses during ALS progression

We examined the correlation between C9orf72 reactivity and biological and clinical variables for individuals with ALS. No significant difference in total C9orf72 reactivity was found between male and female

Table 1 | Epitopes recognized in three or more donors with ALS

Peptide residue	Peptide sequence	Response frequency (%)	Average magnitude
41–55	VRHIWAPKTEQVLLS	3/22 (14%)	96
56–70	DGEITFLANHTLNGE	7/22 (32%)	1,216
61–75	FLANHTLNGEILRNA	3/22 (14%)	462
76–90	ESGAIDVKFFVLSEK	4/22 (18%)	119
81–95	DVKFFVLSEKGVIIV	5/22 (23%)	308
126–140	PLHRVCVDRLTHIIR	3/20 (15%)	133
266–280	CEAESSFKYESGLFV	3/25 (12%)	165
276–290	SGLFVQGLLKDSTGS	4/25 (16%)	87
281–295	QGLLKDSTGSFVLPF	4/25 (16%)	273
361–375	TPDLNIFQDVLHRDT	3/20 (15%)	107
366–380	IFQDVLHRDTLVKAF	6/20 (30%)	181
376–390	LVKAFLDQVFQLKPG	3/20 (15%)	50
381–395	LDQVFQLKPGLSLRS	3/20 (15%)	470
391–405	LSLRSTFLAQFLLVL	3/19 (16%)	568
396–410	TFLAQFLLVLHRKAL	4/19 (21%)	632
401–415	FLLVLHRKALTLIKY	4/19 (21%)	657
406–420	HRKALTLIKYIEDDT	3/19 (16%)	472
411–425	TLIKYIEDDTQKGKK	3/19 (16%)	253
421–435	QKGKKPFKSLRNLKI	4/19 (21%)	769
426–440	PFKSLRNLKIDLDLT	3/19 (16%)	871
426–440[a]	PFKSLRNLKIDLDLT[a]	5/19 (26%)	500
431–445	RNLKIDLDLTAEGDL	3/19 (16%)	375
431–445[a]	RNLKIDLDLT[a]AEGDL	5/19 (26%)	718

Peptides associated with three or more positive responses are shown. Sequence positions, sequence, frequency of responses and average magnitude (total spot-forming cells (SFCs) per 10^6 PBMCs for each donor tested) are shown. [a]Phosphorylated peptides.

Table 2 | HLA-restricted C9orf72 peptides and corresponding HLA alleles

Peptide sequence	Allele	RATE *P* value	Binding percentile rank[a]
VRHIWAPKTEQVLLS	DRB1*14:01	0.025	29
TPDLNIFQDVLHRDT	DRB1*01:02	0.022	20
LDQVFQLKPGLSLRS	DRB1*01:02	0.022	3.3
IFQDVLHRDTLVKAF	DRB1*03:01	0.028	4.9
HRKALTLIKYIEDDT	DQB1*05:01	0.050	22
PFKSLRNLKIDLDLT	DQB1*05:01	0.050	11
RNLKIDLDLTAEGDL	DQB1*05:01	0.050	12

[a]Binding percentile rank was determined using the NetMHCIIpan-4.1 EL algorithm[26]; a small number indicates high affinity.

individuals (Extended Data Fig. 6a). In addition, no significant correlation was found between total C9orf72 reactivity and age (Extended Data Fig. 6b), time from symptom onset (Extended Data Fig. 6c) or time from diagnosis (Extended Data Fig. 6d). No significant difference was also noted for any individual cytokine considered separately (not shown). A trend for a positive correlation was found between IL-5 responses and ALSFRS-R score ($r = 0.279$, $P = 0.119$), whereas no trend between IFNγ and IL-10 responses and ALSFRS-R was detected (Extended Data Fig. 6e–h). Thus, this suggests that C9orf72 reactivity is present at disease onset and diagnosis.

C9orf72 responsiveness and C9orf72 mutations

Because ALS is associated with multiple genes, we investigated whether differences in C9orf72 reactivity were associated with specific mutant alleles that have been linked to the disease. Notably, C9orf72 $CD4^+$ T cell reactivity was approximately sixfold higher in individuals carrying mutations in the non-coding regions of C9orf72 than it was in individuals with ALS who had other mutations (ataxin-2, CHCHD10, FIG4, NEK1, SOD1 and TBK1), or in those who did not carry known mutations or for whom genetic data were not available (unknown mutation status) (Extended Data Fig. 6i; $P = 0.011$). The difference was most pronounced for IL-5 and IL-10; IFNγ showed a non-significant trend (Extended Data Fig. 6j–l; $P = 0.024$, $P = 0.004$ and $P = 0.175$, respectively). We validated these findings in a second cohort of seven participants with ALS carrying the C9orf72 mutation and seven participants with ALS who did not carry any known mutations linked with ALS (Extended Data Table 3). In this completely independent cohort, overall C9orf72 $CD4^+$ T cell reactivity was more than 15-fold higher in individuals carrying mutations in the non-coding regions of C9orf72 (Fig. 4a). T cell responses towards C9orf72 were increased in the C9orf72 mutation carriers for all three cytokines in the validation cohort (Fig. 4b–d).

C9orf72 responsiveness and survival time

For a subset of the patients, the expected survival time was predicted using the ENCALS prediction model[31]. Using this approach, we categorized patients according to their predicted survival time: very short (one individual), short (one individual), intermediate (four individuals), long (three individuals) or very long (eight individuals). Notably, we observed an approximately fivefold higher IL-10-mediated T cell response towards C9orf72 in individuals with ALS who had a longer predicted survival time (long to very long; 43.7 and 91.0 months median predicted survival time, respectively, in the original study[31]), compared with patients who had a shorter predicted survival time (very short to intermediate; 17.7, 25.3 and 32.2 months median predicted survival time, respectively, in the original study[31]) ($P = 0.033$; Fig. 4e–h).

Discussion

Here we identify C9orf72 as a major target of ALS-associated T cell autoreactivity. This is, to our knowledge, the first study showing the recognition by human T cells of a specific autoantigen associated with ALS. Notably, although the autoreactive T cell response is found broadly in individuals with ALS, it is particularly high in those who are carriers of C9orf72 mutant alleles in classically non-coding regions of the open reading frame. We find that the T cell subset associated with C9orf72 reactivity predominantly comprises $CD4^+$ T cells associated with both inflammatory and anti-inflammatory phenotypes. The anti-inflammatory IL-10-mediated responses were associated with a longer predicted survival time, raising the possibility that enhancing this anti-inflammatory component might provide therapeutic benefits. The responses were broad, encompassing several unique T cell epitopes.

Neurodegenerative diseases such as PD and AD were classically not considered to have autoimmune features. However, multiple sclerosis (MS) is associated with high levels of brain infiltration of T cells suspected to react with epitopes derived from viral-related or myelin-related proteins[32]. Adaptive immune responses related to herpes viruses have been implicated in AD pathogenesis[33]. We have also reported that people with PD have $CD4^+$ and $CD8^+$ T cells that react with α-syn and PINK1, products of PD-associated genes[7,18,20]. Thus, the involvement of adaptive immune responses in neurodegenerative disease might be common rather than exceptional.

We identify autoimmune responses to epitopes derived from C9orf72, a protein corresponding to the most common genetic cause of ALS[10]. C9orf72 is thought to have roles in regulating autophagy and

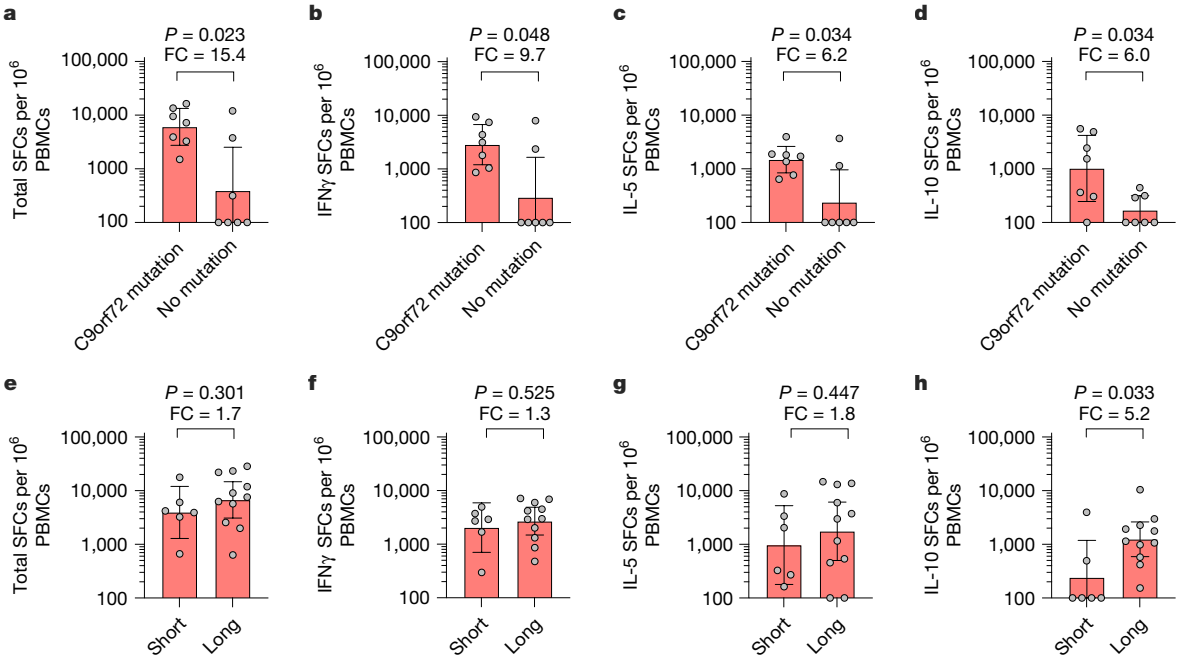

Fig. 4 | IL-5- and IL-10-mediated T cell responses are associated with C9orf72 mutation status and predicted survival. a–**d**, Total (**a**), IFNγ-mediated (**b**), IL-5-mediated (**c**) and IL-10-mediated (**d**) T cell responses towards C9orf72 in a validation cohort of participants with ALS carrying the C9orf72 mutation ($n = 7$) or not carrying any mutation linked to an increased risk of ALS ($n = 7$). **e**–**h**, Total (**e**), IFNγ-mediated (**f**), IL-5-mediated (**g**) and IL-10-mediated (**h**) T cell responses towards C9orf72 in individuals with ALS with a short ($n = 6$) or long ($n = 11$) predicted survival time. *P* values from two-tailed Mann–Whitney tests and geometric mean ± 95% confidence intervals are shown.

secretory pathways[13]. In PD, AD and ALS, disruption of autophagy and intracellular transport has been found to induce increased autophagic organelle fusion with the plasma membrane and secretion of contents into the extracellular space by neurons through a process known as secretory autophagy[29,34,35]. These secreted exosomes have been found to be enriched for proteins involved in autophagy[30]. Because C9orf72 is involved in autophagy, it is possible that HLA-II-expressing cells of the monocyte lineage, such as astrocytes, microglia and border-associated macrophages, could internalize extracellular C9orf72-containing autophagosome content, and present C9orf72 antigens for recognition by $CD4^+$ T cells. Alternatively, C9orf72 could be released during neuronal cell death, and thereafter internalized by glial cells or central nervous system (CNS)-associated macrophages and presented to $CD4^+$ T cells. Because both neuronal cell death and secretory autophagy are increased in PD, AD and ALS, this could explain why individuals with PD and AD were also found to have increased T cell responses towards C9orf72. However, the phenotype of C9orf72-reactive T cells differed between individuals with ALS, those with PD and those with AD, in that individuals with PD or AD had a significantly higher proportion of pro-inflammatory IFNγ-releasing cells and lower proportion of IL-5-releasing cells than individuals with ALS. The underlying mechanisms that drive this difference in T cell phenotype are not known, but it will be of interest in future studies to investigate whether IL-10-releasing C9orf72-specific T cells could provide a therapeutic approach in PD and AD, as the results here suggest for ALS. Future studies will aim to establish whether and how regulatory C9orf72-specific T cells can slow the progression of ALS in preclinical animal models; for example, considering whether regulatory C9orf72-specific T cells promote a neuroprotective phenotype in antigen-presenting glial cells[36]. However, to the best of our knowledge, such a model is not at present available.

We did not detect significant differences in SOD1-specific T cell responses, and observed only a non-significant trend in total reactivity for TDP-43, consistent with two previous studies that found a lack of T cell reactivity with TDP-43 in individuals with ALS[8,9]. We did, however, detect a small but significant increase in IL-5-mediated T cell responses towards TDP-43. Thus, although TDP-43 does not seem to be a major target of autoreactive T cells in ALS, it could potentially be a target of autoreactive T cells in a subset of patients. Our results, therefore, do not exclude the possibility of additional autoimmune targets in ALS, and we note that individuals with disorders such as PD and MS have been found to have multiple autoimmune antigens[7,18,37]. Previous studies have reported that individuals with ALS have increased frequencies of clonally expanded T cells[8,38], including T_H2-like T cells in the cerebrospinal fluid[38]. However, because no previous studies have reported a target of these expanded cells, it is not known whether this expansion is driven by an autoimmune process, or through bystander activation owing to increased levels of inflammatory cytokines.

We find that the targets of T cell reactivity cover the length of the C9orf72 protein, with regions spanning residues 41–95, 266–295 and 361–445 associated with high immunogenicity. Notably, the finding that the reactivity spans across C9orf72 argues against a molecular mimicry effect, as suggested for MS, in which T cells reactive for EBV also cross-react with myelin autoantigens[32]. Moreover, the observation that individuals with ALS have T cell reactivity towards a median of 3 epitopes, and as many as 26 peptides, indicates that they typically have an oligoclonal—and, in some individuals, polyclonal—T cell response to C9orf72. Analysis of predicted HLA-binding capacity reveals a possible mechanism for the high immunogenicity of C9orf72, in that these regions contain peptides with the capacity to bind multiple HLA types that are commonly encountered in human populations[39]. Notably, the regions do not overlap with the C9orf72 region that carries the hexanucleotide repeat expansion associated with increased disease susceptibility, which is in the first intronic region[40]. In addition to the formation of dipeptides due to the high repeat number of the hexanucleotide repeat expansion sequence, which might affect proteostasis, the C9orf72 mutation is associated with TDP-43 mislocalization[41], the presence of nuclear RNA foci[10,11], cytoplasmic stress granules and reduced expression of the C9orf72 protein[13]. As C9orf72 is highly expressed in $CD14^+$ conventional monocytes[13,42], reduced expression might result in reduced peripheral tolerance towards C9orf72.

The loss of peripheral tolerance would allow C9orf72-specific T cells to persist and later expand in individuals with ALS when extracellular C9orf72-containing autophagosome content is internalized and presented to T cells by microglia or other antigen-presenting cells in the CNS. Consistent with this hypothesis, we found, in two independent cohorts, that individuals with ALS who carry the C9orf72 intron mutation have the highest autoimmune C9orf72-specific T cell responses. Individuals with long predicted survival times exhibited the highest IL-10-mediated T cell responses, suggesting that T cell responses skewed away from IL-10 are associated with a more rapid disease progression. As ALS is associated with decreased C9orf72 expression[13], it is possible that a pro-inflammatory autoimmune attack on C9orf72 results in decreased expression and thereby influences pathogenesis.

Although neurons and oligodendrocytes do not typically present antigens, and CNS parenchymal T cells are rare in healthy conditions, rat motor neurons have been shown to express MHC class I RNA and to upregulate this expression with exposure to IFNγ (ref. 43). CD8 T cells expressing mutant SOD1 have been reported to kill motor neurons in mice[44]. In the mouse CNS, IFNγ rapidly promotes a high level of MHC class I synthesis in oligodendrocytes and microglia, with lower levels in neurons and astrocytes[45], and HLA class II expression has been reported in classes of human oligodendrocytes[46].

The T cells that recognize C9orf72 are predominantly $CD4^+$, with a tendency for polarization toward a T_H2 cell or regulatory T (T_{reg}) cell-like phenotype. Individuals with ALS have substantially more C9orf72-reactive T cells than healthy controls, but they have a lower proportion of T_H1- and T_H1*-like $CD4^+$ T cells and a higher frequency of T_H2- and T_{reg}-like T cells than control individuals. Of note, this was specific for the C9orf72-reactive T cells, because no difference in the frequency of IL-5- or IL-10-releasing cells was observed in response to the control antigen EBV. IL-5 and IL-10 are associated with anti-inflammatory features[47], and it is possible that the autoimmune reactivity detected might be multifaceted, with an IFNγ component having an inflammatory role and an IL-10 component a counter-inflammatory one. Although IL-5 and other T_H2-associated cytokines have classically been associated with allergy and thought to act principally on basophils, these cytokines have also been found to have crucial roles in the regulation of cognitive function and brain inflammatory processes[47]. We found that the IFNγ-releasing T cells had a lower functional avidity to the C9orf72 peptides in participants with ALS than in healthy controls. It is tempting to speculate that this reduced avidity reflects an increased peripheral tolerance towards C9orf72 mediated by the IL-10-releasing T cells, but this needs to be further investigated. The observation that IL-10-mediated C9orf72-specific T cell responses were significantly higher in participants with ALS who had longer predicted survival times aligns with previous reports suggesting that ALS is characterized by an initial neuroprotective T_H2 and T_{reg} cell response, which is subsequently replaced by a pro-inflammatory T_H1 response[38,48,49]. Those studies were limited to bulk phenotyping of T cells[38,49,50], and the identification of C9orf72 as a major target of ALS-associated T cell autoreactivity promises to help define the specific changes in the adaptive immune system that occur over the course of the disease. Overall, our findings support suggestions that neuronal and oligodendrocyte death in ALS could be due to an imbalance of neuroinflammatory and counter-inflammatory pathways[4], and are in line with reports of high levels of effector T cells[38,50]. Given this, clinical trials intended to enhance T_{reg} cells should be considered[5]—in particular, trials of antigen-specific T cell responses, which could provide targeted therapies for people with ALS.

Limitations of the study

This study has several limitations. Because of the low frequency of autoreactive T cells, our experiments required an in vitro restimulation step to expand the relatively rare responding T cells[7,18,20] so as to obtain sufficient cells for a reliable phenotyping. Our study did not use tetramer staining reagents: unlike the peptide pool approach, the design of HLA tetramers requires a priori knowledge of the specific epitopes to which an individual responds and the HLA background of the individual. The use of this technique is therefore limited to epitopes that are already well characterized. Furthermore, historically, producing effective HLA class II tetramers, which are required to measure responses by CD4 T cells, has been technically challenging. However, analysing potential HLA restrictions for selected epitopes could enable the design of tetramer reagents in future studies.

Owing to the low responses of control individuals to the C9orf72 peptide pool, we did not perform peptide–response deconvolution for these participants. The study did not address phenotypic subtypes of ALS or related disorders, including frontotemporal dementia. As mentioned, as with most autoimmune disorders, there are likely to be additional targets of autoimmune reactivity. This study examined a limited number of candidate proteins because of their established genetic connections with ALS. It would be interesting to perform an unbiased analysis of candidate proteins. In our approach, each candidate antigen is tested with sets of overlapping 15-mer peptides, and to test, for example, the top 1,000 candidate open reading frames expressed in nervous tissues, hundreds of thousands of peptides would be required. Because about two million to three million cells (corresponding to 2–3 ml of blood) are required to measure the rare autoimmune T cells that respond to any given peptide pool, testing even 1,000 candidates would require the donation of an impractical amount of blood. T cell-receptor analysis of antigen-specific T cells in the CNS would be valuable, but T cells are present at very low numbers in the CNS of people with ALS[38], and a successful single-cell characterization of antigen-specific T cells in tissue requires thousands of cells.

Online content

Any methods, additional references, Nature Portfolio reporting summaries, source data, extended data, supplementary information, acknowledgements, peer review information; details of author contributions and competing interests; and statements of data and code availability are available at https://doi.org/10.1038/s41586-025-09588-6.

1. Kawamata, T., Akiyama, H., Yamada, T. & McGeer, P. L. Immunologic reactions in amyotrophic lateral sclerosis brain and spinal cord tissue. *Am. J. Pathol.* **140**, 691–707 (1992).
2. Engelhardt, J. I., Tajti, J. & Appel, S. H. Lymphocytic infiltrates in the spinal cord in amyotrophic lateral sclerosis. *Arch. Neurol.* **50**, 30–36 (1993).
3. Rodrigues Lima-Junior, J., Sulzer, D., Lindestam Arlehamn, C. S. & Sette, A. The role of immune-mediated alterations and disorders in ALS disease. *Hum. Immunol.* **82**, 155–161 (2021).
4. Appel, S. H., Beers, D. R. & Zhao, W. Amyotrophic lateral sclerosis is a systemic disease: peripheral contributions to inflammation-mediated neurodegeneration. *Curr. Opin. Neurol.* **34**, 765–772 (2021).
5. Thonhoff, J. R. et al. Combined regulatory T-lymphocyte and IL-2 treatment Is safe, tolerable, and biologically active for 1 year in persons with amyotrophic lateral sclerosis. *Neurol. Neuroimmunol. Neuroinflamm.* **9**, e200019 (2022).
6. Murray, M. E. et al. Clinical and neuropathologic heterogeneity of c9FTD/ALS associated with hexanucleotide repeat expansion in *C9ORF72*. *Acta Neuropathol.* **122**, 673–690 (2011).
7. Sulzer, D. et al. T cells from patients with Parkinson's disease recognize α-synuclein peptides. *Nature* **546**, 656–661 (2017).
8. Campisi, L. et al. Clonally expanded CD8 T cells characterize amyotrophic lateral sclerosis-4. *Nature* **606**, 945–952 (2022).
9. Ramachandran, S. et al. Low T-cell reactivity to TDP-43 peptides in ALS. *Front. Immunol.* **14**, 1193507 (2023).
10. DeJesus-Hernandez, M. et al. Expanded GGGGCC hexanucleotide repeat in noncoding region of *C9ORF72* causes chromosome 9p-linked FTD and ALS. *Neuron* **72**, 245–256 (2011).
11. Renton, A. E. et al. A hexanucleotide repeat expansion in *C9ORF72* is the cause of chromosome 9p21-linked ALS-FTD. *Neuron* **72**, 257–268 (2011).
12. Sultana, J. et al. C9orf72-associated dipeptide repeat expansions perturb ER–Golgi vesicular trafficking, inducing Golgi fragmentation and ER stress, in ALS/FTD. *Mol. Neurobiol.* **61**, 10318–10338 (2024).
13. Smeyers, J., Banchi, E.-G. & Latouche, M. C9ORF72: what it is, what it does, and why it matters. *Front. Cell. Neurosci.* **15**, 661447 (2021).
14. Longinetti, E. & Fang, F. Epidemiology of amyotrophic lateral sclerosis: an update of recent literature. *Curr. Opin. Neurol.* **32**, 771–776 (2019).

15. McCombe, P. A., Lee, J. D., Woodruff, T. M. & Henderson, R. D. The peripheral immune system and amyotrophic lateral sclerosis. *Front. Neurol.* **11**, 279 (2020).
16. Lindestam Arlehamn, C. S. et al. T-cell deficiency and hyperinflammatory monocyte responses associate with *Mycobacterium avium* complex lung disease. *Front. Immunol.* **13**, 1016038 (2022).
17. Acosta-Rodriguez, E. V. et al. Surface phenotype and antigenic specificity of human interleukin 17-producing T helper memory cells. *Nat. Immunol.* **8**, 639–646 (2007).
18. Williams, G. P. et al. PINK1 is a target of T cell responses in Parkinson's disease. *J. Clin. Invest.* **135**, e180478 (2024).
19. da Silva Antunes, R. et al. The MegaPool approach to characterize adaptive CD4$^+$ and CD8$^+$ T cell responses. *Curr. Protoc.* **3**, e934 (2023).
20. Lindestam Arlehamn, C. S. et al. α-Synuclein-specific T cell reactivity is associated with preclinical and early Parkinson's disease. *Nat. Commun.* **11**, 1875 (2020).
21. Dan, J. M. et al. A cytokine-independent approach to identify antigen-specific human germinal center T follicular helper cells and rare antigen-specific CD4$^+$ T cells in blood. *J. Immunol.* **197**, 983–993 (2016).
22. Dunmire, S. K., Verghese, P. S. & Balfour, H. H. Primary Epstein–Barr virus infection. *J. Clin. Virol.* **102**, 84–92 (2018).
23. McKhann, G. et al. Clinical diagnosis of Alzheimer's disease: report of the NINCDS-ADRDA Work Group under the auspices of Department of Health and Human Services Task Force on Alzheimer's Disease. *Neurology* **34**, 939–944 (1984).
24. McKhann, G. M. et al. The diagnosis of dementia due to Alzheimer's disease: recommendations from the National Institute on Aging–Alzheimer's Association workgroups on diagnostic guidelines for Alzheimer's disease. *Alzheimers Dement.* **7**, 263–269 (2011).
25. Paul, S. et al. Experimental validation of the RATE tool for inferring HLA restrictions of T cell epitopes. *BMC Immunol.* **18**, 20 (2017).
26. Reynisson, B., Alvarez, B., Paul, S., Peters, B. & Nielsen, M. NetMHCpan-4.1 and NetMHCIIpan-4.0: improved predictions of MHC antigen presentation by concurrent motif deconvolution and integration of MS MHC eluted ligand data. *Nucleic Acids Res.* **48**, W449–w54 (2020).
27. Nilsson, J. B. et al. Accurate prediction of HLA class II antigen presentation across all loci using tailored data acquisition and refined machine learning. *Sci. Adv.* **9**, eadj6367 (2023).
28. Greenbaum, J. et al. Functional classification of class II human leukocyte antigen (HLA) molecules reveals seven different supertypes and a surprising degree of repertoire sharing across supertypes. *Immunogenetics* **63**, 325–335 (2011).
29. Hartmann, J. et al. SKA2 regulated hyperactive secretory autophagy drives neuroinflammation-induced neurodegeneration. *Nat. Commun.* **15**, 2635 (2024).
30. Palumbos, S. D., Popolow, J., Goldsmith, J. & Holzbaur, E. L. F. Autophagic stress activates distinct compensatory secretory pathways in neurons. *Proc. Natl Acad. Sci. USA* **122**, e2421886122 (2025).
31. Westeneng, H. J. et al. Prognosis for patients with amyotrophic lateral sclerosis: development and validation of a personalised prediction model. *Lancet Neurol.* **17**, 423–433 (2018).
32. Bjornevik, K., Münz, C., Cohen, J. I. & Ascherio, A. Epstein–Barr virus as a leading cause of multiple sclerosis: mechanisms and implications. *Nat. Rev. Neurol.* **19**, 160–171 (2023).
33. Gate, D. et al. Clonally expanded CD8 T cells patrol the cerebrospinal fluid in Alzheimer's disease. *Nature* **577**, 399–404 (2020).
34. Iguchi, Y. et al. Exosome secretion is a key pathway for clearance of pathological TDP-43. *Brain* **139**, 3187–3201 (2016).
35. Sepúlveda, D., Cisternas-Olmedo, M., Arcos, J., Nassif, M. & Vidal, R. L. Contribution of autophagy–lysosomal pathway in the exosomal secretion of α-synuclein and its impact in the progression of Parkinson's disease. *Front. Mol. Neurosci.* **15**, 805087 (2022).
36. Calafatti, M., Cocozza, G., Limatola, C. & Garofalo, S. Microglial crosstalk with astrocytes and immune cells in amyotrophic lateral sclerosis. *Front. Immunol.* **14**, 1223096 (2023).
37. Bronge, M. et al. Identification of four novel T cell autoantigens and personal autoreactive profiles in multiple sclerosis. *Sci. Adv.* **8**, eabn1823 (2022).
38. Yazdani, S. et al. T cell responses at diagnosis of amyotrophic lateral sclerosis predict disease progression. *Nat. Commun.* **13**, 6733 (2022).
39. Oseroff, C. et al. Molecular determinants of T cell epitope recognition to the common Timothy grass allergen. *J. Immunol.* **185**, 943–955 (2010).
40. Balendra, R. & Isaacs, A. M. *C9orf72*-mediated ALS and FTD: multiple pathways to disease. *Nat. Rev. Neurol.* **14**, 544–558 (2018).
41. Cook, C. N. et al. *C9orf72* poly(GR) aggregation induces TDP-43 proteinopathy. *Sci. Transl. Med.* **12**, eabb3774 (2020).
42. Rizzu, P. et al. *C9orf72* is differentially expressed in the central nervous system and myeloid cells and consistently reduced in *C9orf72, MAPT* and *GRN* mutation carriers. *Acta Neuropathol. Commun.* **4**, 37 (2016).
43. Linda, H., Hammarberg, H., Piehl, F., Khademi, M. & Olsson, T. Expression of MHC class I heavy chain and β2-microglobulin in rat brainstem motoneurons and nigral dopaminergic neurons. *J. Neuroimmunol.* **101**, 76–86 (1999).
44. Coque, E. et al. Cytotoxic CD8$^+$ T lymphocytes expressing ALS-causing SOD1 mutant selectively trigger death of spinal motoneurons. *Proc. Natl Acad. Sci. USA* **116**, 2312–2317 (2019).
45. Hobson, B. D. et al. Conserved and cell type-specific transcriptional responses to IFN-γ in the ventral midbrain. *Brain Behav. Immun.* **111**, 277–291 (2023).
46. Jakel, S. et al. Altered human oligodendrocyte heterogeneity in multiple sclerosis. *Nature* **566**, 543–547 (2019).
47. Mamuladze, T. & Kipnis, J. Type 2 immunity in the brain and brain borders. *Cell. Mol. Immunol.* **20**, 1290–1299 (2023).
48. Beers, D. R. et al. Neuroinflammation modulates distinct regional and temporal clinical responses in ALS mice. *Brain Behav. Immun.* **25**, 1025–1035 (2011).
49. Jin, M., Günther, R., Akgün, K., Hermann, A. & Ziemssen, T. Peripheral proinflammatory Th1/Th17 immune cell shift is linked to disease severity in amyotrophic lateral sclerosis. *Sci. Rep.* **10**, 5941 (2020).
50. Rolfes, L. et al. Amyotrophic lateral sclerosis patients show increased peripheral and intrathecal T-cell activation. *Brain Commun.* **3**, fcab157 (2021).

Methods

Study approval

All participants provided written informed consent for participation in the study. Ethical approval was obtained from the Institutional Review Boards at La Jolla Institute for Immunology (protocol numbers VD-124, VD-118, VD-155 and VD-171), Massachusetts General Hospital (protocol number 2006P000982), Emory University (protocol number CR003-IRB00078771), University of California, Irvine (protocol number 20163191), National Institutes of Health (protocol number 17N0131), University of California, San Diego (protocol number 120295) and Columbia University Irving Medical Center (CUMC; protocol numbers IRB-AAAQ9714 and AAAS1669). Research activities with samples from Sanguine Biosciences (a fee-for-service, contract research organization) are not considered human participants research under Health and Human Services regulations.

Study participants

Individuals with ALS ($n = 40$) and healthy control individuals ($n = 28$) were recruited by Massachusetts General Hospital, Emory University, University of California, Irvine, Sanguine Biosciences and the National Institutes of Health, referred to as the study cohort in the Methods. An additional 14 participants with ALS were included from the University of California, San Diego and served as a validation cohort. Samples from Massachusetts General Hospital were used to perform preliminary experiments and are not included in the data presented in this study. Inclusion criteria for patients with ALS consisted of: (i) a diagnosis of familial or sporadic ALS according to the El Escorial criteria; (ii) aged 20 years or older at the time of symptom onset; and (iii) the ability to provide informed consent. Exclusion criteria included: (i) other major neurological or medical diseases that could cause progressive weakness or cognitive dysfunction; and (ii) an unstable medical condition that would make participation unsafe. Inclusion criteria for age- and sex-matched control individuals consisted of: (i) age including 53–82 to match the ages of individuals with ALS; (ii) sex matching that of individuals with ALS; and (iii) the ability to provide informed consent. Exclusion criteria for control participants were the same as those for ALS, with the addition of self-reported ALS genetic risk factors (that is, ALS in first-degree blood relatives). ALS diagnosis was based on clinical criteria (symptoms and examination findings). Typically, the diagnosis was associated with clinical findings of upper and lower motor dysfunction, a progressive course and a failure of diagnostic tests such as brain and spinal cord magnetic resonance imaging (MRI), electrophysiological testing and routine laboratory studies to identify an alternative cause. If the clinical presentation deviated from these typical features, a neuromuscular specialist with extensive experience in diagnosing ALS was consulted to adjudicate the diagnosis.

Specific clinical information on the participants with ALS was collected, including age and sex, the time since ALS symptom onset, the time when the individual started experiencing symptoms related to their ALS diagnosis, the time after ALS diagnosis and the time of donation after the initial diagnosis of ALS to understand the duration of the disease (Table 1). ALSFRS-R data were used to evaluate the functional status of participants with ALS and monitor functional changes in patients over time. ALSFRS-R data were missing for 7 participants with ALS from the study cohort and all 14 patients from the validation cohort; these were excluded from analyses in which the ALSFRS-R was used. Predicted survival time was obtained using the online ENCALS prediction model[31] (http://tool.encalssurvivalmodel.org/), a well-established and widely used survival prediction tool for participants with ALS, originally developed using data from more than 10,000 individuals across several ALS centres in Europe. The classification is based on diagnostic delay (months), progression rate (points decrease on ALSFRS-R per month), forced vital capacity (percentage of predicted capacity based on normative values for sex, age and height), definite ALS (according to El Escorial criteria), frontotemporal dementia (yes or no), C9orf72 repeat expansion (yes or no) and site of onset. The prediction model classifies patients into one of five categories on the basis of predicted survival time: very short, short, intermediate, long or very long. Genetic mutations were noted on an individual basis if genetic sequencing was performed. Twenty-four individuals with ALS were HLA-typed at an American Society for Histocompatibility and Immunogenetics (ASHI)–accredited laboratory at Murdoch University in Western Australia. Typing for HLA class II (DQA1, DQB1, DRB1, DRB3, DRB4, DRB5 and DPB1) was performed using locus-specific PCR amplification, sequencing was done using the Illumina MiSeq platform and the alleles were called using an ASHI-accredited HLA allele caller software pipeline, IIID HLA analysis suite (http://www.iiid.com.au/laboratory-testing/). The full HLA typing data for these patients are provided in Supplementary Table 2.

Individuals with PD ($n = 15$) were recruited by the Movement Disorders Clinic at the Department of Neurology at CUMC. Inclusion criteria for the patients consisted of (i) clinically diagnosed PD with the presence of bradykinesia and either resting tremor or rigidity; (ii) PD diagnosis between the age of 35 and 80; (iii) history establishing the benefit of dopaminergic medication; and (iv) ability to provide informed consent. Exclusion criteria for PD were: (i) atypical parkinsonism or other neurological disorders; (ii) history of cancer within the past three years; (iii) autoimmune disease; and (iv) chronic immune-modulatory therapy. The recruited individuals with PD all met the UK Parkinson's Disease Society Brain Bank criteria for PD.

Individuals with AD ($n = 15$) were recruited from the Alzheimer's Disease Research Center at CUMC or from PrecisionMed (a fee-for-service, contract research organization). Patients recruited from CUMC were diagnosed by neurologists according to the National Institute of Aging and Alzheimer's Association criteria[24]; those recruited from PrecisionMed were diagnosed according to NINCDS-ADRDA criteria[23], by a neurologist or internist. The donors with AD and those with PD were selected to be age- and sex-matched to the donors with ALS.

Isolation of PBMCs

Venous blood was collected from each participant in either heparin or EDTA-containing blood bags or tubes, as previously reported and described. PBMCs were isolated from whole blood by density-gradient centrifugation using Ficoll Paque Plus (GE). In brief, blood was first spun at 800*g* for 15 min with brakes off to remove plasma. Plasma-depleted blood was then diluted with RPMI, and 35 ml of blood was carefully layered on tubes containing 15 ml Ficoll Paque Plus. These tubes were centrifuged at 800*g* for 25 min with the brakes off. The interphase cell layer resulting from this spin was collected, washed with RPMI, counted and cryopreserved in 90% v/v fetal bovine serum (FBS) and 10% v/v dimethyl sulfoxide (DMSO), and stored in liquid nitrogen until tested. The detailed protocol for PBMC isolation can be found at protocols.io (https://doi.org/10.17504/protocols.io.bw2ipgce).

Antigen pools

Sets of overlapping peptides spanning the sequences of TDP-43 (101 peptides; NCBI ABO32290.1), SOD1 (29 peptides; UniProt ID P00441), and C9orf72 antigens (100 peptides; UniProt ID Q96LT7). A previously described[21] pool encompassing EBV epitopes was used as a control. Peptides were synthesized commercially as crude material on a 1-mg scale by TC Peptide Lab. Lyophilized peptide products were dissolved in 100% DMSO at a concentration of 20 mg ml^{-1}, and their quality was spot-checked by mass spectrometry. These peptides were also combined in 'megapools' as described[19] and used in the antigen screening experiments. C9orf72 peptides were also tested individually, as described in the main text.

In vitro expansion of antigen-specific cells and FluoroSpot assay

In vitro expansion and subsequent FluoroSpot assays were performed as previously described[20]. An equal number of ALS and control samples

were included per experiment, to reduce the risk of technical biases. The ALS and control donors were randomly assigned to the individual experimental groups. In brief, PBMCs were thawed and then stimulated with neuroantigen or EBV peptide pools (5 μg ml^{-1}) for four days. After four days, cells were supplemented with fresh RPMI and IL-2 (10 U ml^{-1}, ProspecBio), and fed again every three days until day 11. After two weeks of culture, T cell responses to neuroantigen pools were measured by IFNγ, IL-5 and IL-10 FluoroSpot assays. Plates (Mabtech) were coated overnight at 4 °C with an antibody mixture of mouse anti-human IFNγ (clone 1-D1K, Mabtech), mouse anti-human IL-5 (clone TRFK5, Mabtech) and mouse anti-human IL-10 (clone 9D7, Mabtech). A total of 1×10^5 of the collected cells were plated in each well of the coated FluoroSpot plates along with each respective antigen (5 μg ml^{-1}), and incubated at 37 °C in 5% CO_2 for 22 h. Cells were also stimulated with 10 μg ml^{-1} phytohaemagglutinin (positive control) and DMSO corresponding to the concentration in the peptide pool dilutions (negative control) to assess non-specific cytokine production. All conditions were tested in triplicate. After incubation, cells were removed, and membranes were washed. An antibody cocktail containing IFNγ (7-B6-1-FS-BAM), IL-5 (5A10-WASP) and IL-10 (12G8-biotin) prepared in phosphate-buffered saline (PBS) with 0.1% bovine serum albumin was added and incubated for two hours at room temperature. Membranes were then washed again, and secondary antibodies (anti-BAM-490, anti-WASP-640 and SA-550) were incubated for one hour at room temperature. Then, membranes were washed, incubated with fluorescence enhancer (Mabtech) and air-dried for reading. Spots were read and counted using the Mabtech Apex (v.2.0) software on the Mabtech IRIS system. The dilutions of all antibodies used are provided in Supplementary Table 3. Responses were considered positive if they met all three of the following criteria: (i) DMSO background-subtracted SFCs per 10^6 PBMCs ≥ 100; (ii) stimulation index ≥ 2 compared with DMSO controls; and (iii) $P \leq 0.05$ by Student's *t*-test or Poisson distribution test. Negative responses were assigned as 100 SFCs per 10^6 PBMCs, the lower limit of detection of the assay. The total SFCs per donor measurement was obtained by combining the individual IFNγ, IL-5 and IL-10 SFC values for all samples with a positive response. If no positive response was detected for any of the cytokines, the total cytokine response was assigned as 100 SFCs per 10^6 PBMCs. The average cytokine response was calculated by dividing the individual cytokine SFCs by the total SFCs, and the cytokine ratios were calculated by dividing cytokine SFC values.

HLA II binding predictions

The number of predicted binding events of peptides to the 27 most common HLA-DR, HLA-DQ and HLA-DP class II allelic variants was analysed using the MHC-II Binding Prediction Results tool available at the Immune Epitope Database (IEDB)[28]. As suggested by the IEDB, we used the NetMHCIIpan-4.1 EL prediction method, and set the cut-off for a binding event as a predicted binding percentile score threshold of 20% or less[18]. Predicted binding strength was obtained using the NetMHCIIpan-4.1 EL prediction method, and is reported as a normalized rank value compared with peptides from 10,000 randomly selected peptides, with a small value indicating high affinity[25].

Inference of HLA restrictions

HLA restrictions were inferred using RATE, hosted by the IEDB[25]. In brief, RATE infers HLA restrictions by considering the presence or absence of a response to a given epitope as the biological outcome. It calculates the relative frequency of the individuals responding to a given epitope and expressing a given allele, compared with the general test population, and the associated statistical significance. Because spurious results can be observed for HLA alleles in linkage disequilibrium, peptide–HLA associations were validated using the NetMHCIIpan-4.1 EL method, with a percentile score threshold of 30% or less, to validate that the peptides were predicted to bind to their corresponding HLA allele.

Flow cytometry

Spectral methods (Cytek Aurora). Cells were washed, counted and plated in a 96-well plate at a density of 1×10^6 cells per well. Cells were then stained with a mixture of the following antibodies: fixable viability dye eFluor 506 (Thermo Fisher Scientific), CD4-APC-eF780 (clone: RPA-T4, Thermo Fisher Scientific), CD8-BUV496 (clone: RPA-T8, BD Biosciences), CD20-BV563 (clone: 2H7, BD), CD56-APC (clone: 5.1H11, BioLegend), gdTCR-BV421 (clone: 11F2, BD), CCR4-PE Cy-7 (clone: IG1, BD), CD16-PE Cy5 (clone: 3G8, Thermo Fisher Scientific), CD14-BV480 (clone: M5E2, BD), HLA-DR-AF700 (clone: LN3, Thermo Fisher Scientific), CD161-BV650 (clone: DX12, BD), CXCR3-PE (clone: G025H7, BioLegend), CD19-BV605 (clone: HIB19, BioLegend), CD38-PerCP-Cy5.5 (clone: HIT2, BD), CD3-BUV805 (clone: UCHT1, BD), CCR7-BV785 (clone: G043H7, BioLegend), CCR6-BUV395 (clone: 11A, BD), CD26-FITC (clone: BA5b, BioLegend), CD127-PEFire700 (clone: A019D5, BioLegend), CD45-PE Dazzle594 (clone: HI30, BioLegend), CD25-BV711 (clone: M-A251, BioLegend) and CD45RA-BV570 (clone: HI100, BioLegend), for 20 min at 4 °C in the dark. The dilutions of all antibodies used are provided in Supplementary Table 3. Stained cells were washed twice and resuspended in 100 μl PBS to be run on the Cytek Aurora System (Cytek). FCS files produced from the Cytek Aurora flow cytometer, using the SpectroFlo flow cytometry software (Cytek,v.3.3), were then analysed using FlowJo software (v.10.10.0, Tree Star).

ICS methods (Fortessa X-20). Antigen-specific cells were expanded for two weeks as described above. On day 14, cells were washed, counted, plated in a 96-well plate at a density of 1×10^6 cells per well, and restimulated with the C9orf72 megapool. After a two-hour incubation, cells were treated for an additional 4 h with GolgiPlug (BD) and GolgiStop (BD). Cells were then washed and stained with a mixture of the following antibodies: fixable viability dye eFluor 506 (Thermo Fisher Scientific), CD4-APC-eF780 (clone: RPA-T4, Thermo Fisher Scientific), CD3-AF700 (clone: UCHT1, BD) and CD8-BV650 (clone: RPA-T8, BioLegend). Cells were incubated for 30 min at 4 °C. Cells were then washed and fixed and permeabilized using the Cyto-Fast Fix/Perm buffer (BioLegend) for 20 min at room temperature. After permeabilization, cells were stained with the following mixture: IL-10-APC (clone: JES3-19F1, BioLegend), IL-4-BV421 (clone: MD425D2, BioLegend), IFNγ-FITC (clone: 4S.B2, Thermo Fisher Scientific) and IL-17-BV785 (clone: BL168, BioLegend) for 20 min at room temperature in the dark. The dilutions of all antibodies used are provided in Supplementary Table 3. Stained cells were then washed twice and resuspended in 100 μl PBS to be run on the Fortessa X-20 flow cytometer (BD). FCS files produced from the Fortessa X-20, using FACSDiva (v.9.2), were then analysed using FlowJo software. The average proportion of each cytokine for each donor was determined by dividing the frequency of cells releasing each cytokine by the total number of cells releasing any of the three cytokines for each donor.

Statistical analysis

Statistical analyses were performed and graphs were created using GraphPad Prism's descriptive statistics, two-tailed Mann–Whitney test, one-way ANOVA with Dunnett's multiple comparisons test, two-tailed Fisher exact test and Spearman's r test as applicable (GraphPad Prism, v.10).

Reporting summary

Further information on research design is available in the Nature Portfolio Reporting Summary linked to this article.

Data availability

Source data for all figures are provided with this paper. FCS files and FlowJo workspace files have been uploaded to Zenodo: spectral files: https://doi.org/10.5281/zenodo.16749283 (ref. 51); ICS files:

https://doi.org/10.5281/zenodo.16749334 (ref. 52), https://doi.org/10.5281/zenodo.16754553 (ref. 53), https://doi.org/10.5281/zenodo.16754591 (ref. 54) and https://doi.org/10.5281/zenodo.16754609 (ref. 55). Source data are provided with this paper.

Code availability

No codes were used within this study.

51. Michaelis, T., Johansson, E., Sulzer, D. & Sette. Autoimmune response to C9orf72 protein in amyotrophic lateral sclerosis - Spectral data. *Zenodo* https://doi.org/10.5281/zenodo.16749283 (2025).
52. Michaelis, T., Johansson, E., Sulzer, D. & Sette, A. Autoimmune response to C9orf72 protein in amyotrophic lateral sclerosis - ICS data Screen 1. *Zenodo* https://doi.org/10.5281/zenodo.16749334 (2025).
53. Michaelis, T., Johansson, E., Sulzer, D. & Sette, A. Autoimmune response to C9orf72 protein in amyotrophic lateral sclerosis - ICS data Screen 2. *Zenodo* https://doi.org/10.5281/zenodo.16754553 (2025).
54. Michaelis, T., Johansson, E., Sulzer, D. & Sette, A. Autoimmune response to C9orf72 protein in amyotrophic lateral sclerosis - ICS data Screen 3. *Zenodo* https://doi.org/10.5281/zenodo.16754591 (2025).
55. Michaelis, T., Johansson, E., Sulzer, D. & Sette, A. Autoimmune response to C9orf72 protein in amyotrophic lateral sclerosis - ICS data Screen 4. *Zenodo* https://doi.org/10.5281/zenodo.16754609 (2025).

Acknowledgements This work was supported by La Jolla Institute for Immunology, Kyowa Kirin North America, the Swedish Research Council (salary for E.J., grant reference 2024-00175) and the Freedom Together Foundation (to D.S.), and in part by the Intramural Research Program, National Institute of Neurological Disorders and Stroke, National Institutes of Health (A. Snyder, J.C. and J.Y.K.). The contributions of the NIH authors were made as part of their official duties as NIH federal employees, are in compliance with agency policy requirements, and are considered works of the US Government. However, the findings and conclusions presented in this paper are those of the authors and do not necessarily reflect the views of the NIH or the US Department of Health and Human Services.

Author contributions C.S.L.A., D.S. and A. Sette participated in the design and direction of the study. T.M., E.J., J.S. and C.S.L.A. performed and analysed the experiments. A.F., J.D.B., M.C., N.A.G., C.F., A. Snyder, J.Y.K., J.C., J.R. and K.S.M. recruited participants and performed clinical evaluations. E.J.P. and S.A.M. performed HLA typing. T.M., C.S.L.A., E.J., D.S. and A. Sette wrote the manuscript. All authors read, edited and approved the manuscript before submission.

Competing interests The authors have declared that no competing interests exist.

Additional information

Supplementary information The online version contains supplementary material available at https://doi.org/10.1038/s41586-025-09588-6.

Correspondence and requests for materials should be addressed to David Sulzer or Alessandro Sette.

Peer review information *Nature* thanks Aaron Gitler, Lawrence Stern and the other, anonymous, reviewer(s) for their contribution to the peer review of this work.

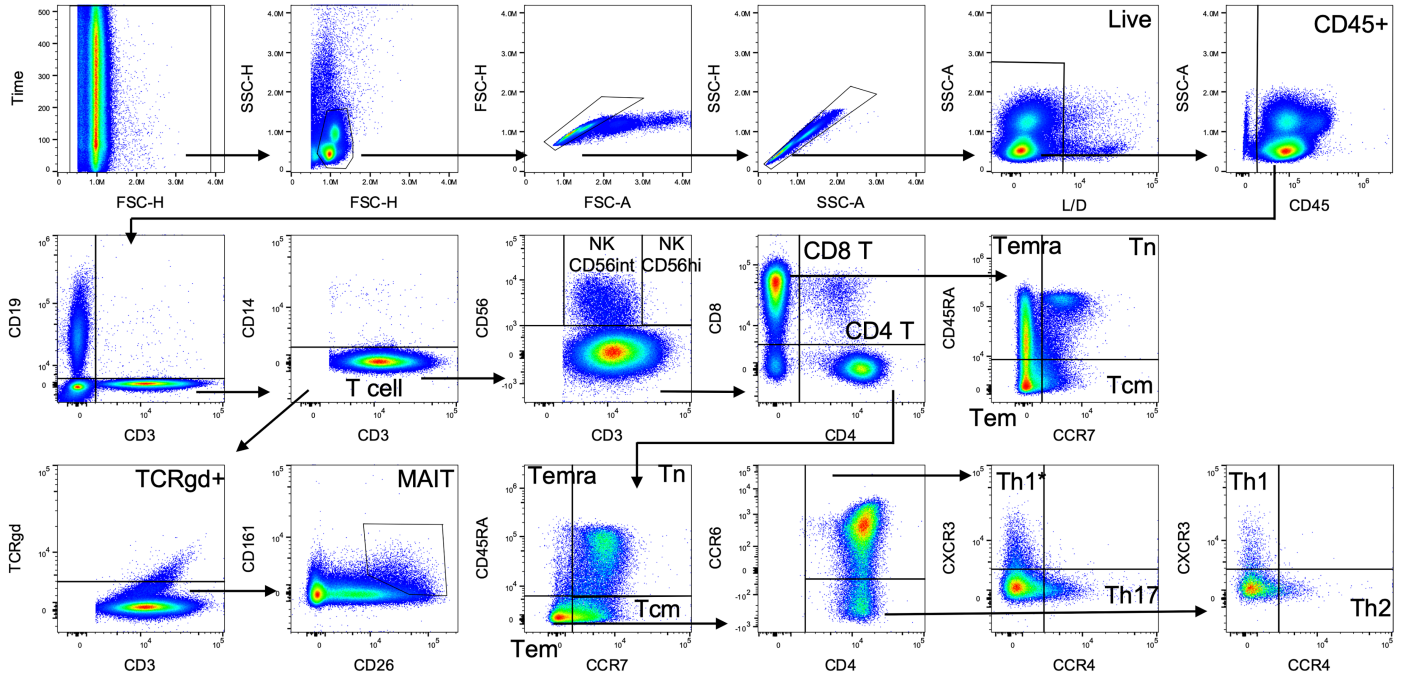

Extended Data Fig. 1 | Gating strategy for flow cytometry. Gating strategies for broad immunophenotyping of T cell subsets in PBMCs. Related to data in Fig. 1.

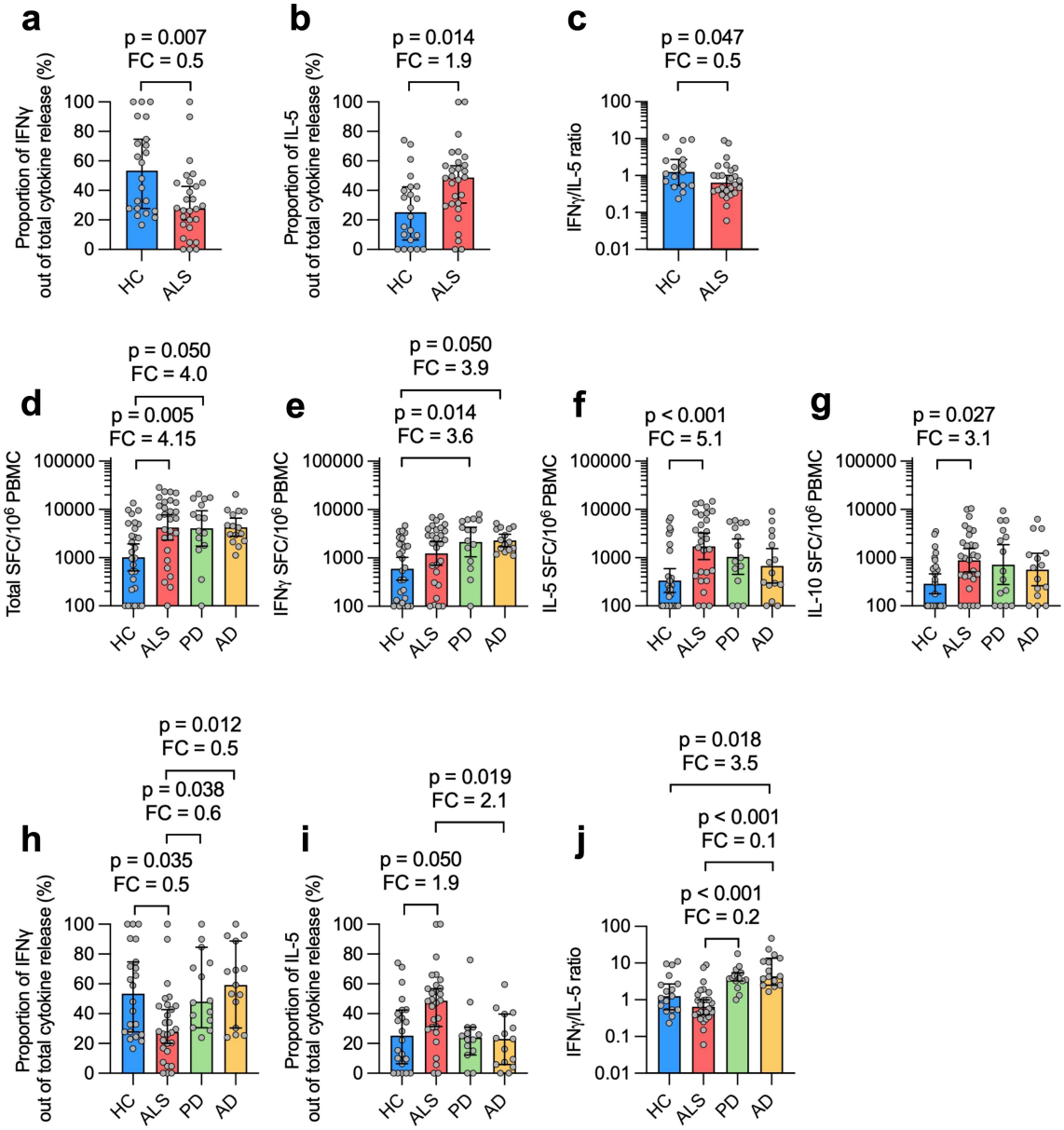

Extended Data Fig. 2 | Donors with ALS have an IL-5-biased T cell response. Proportion of IFNγ (**a**) and IL-5 (**b**) releasing T cells among all cytokine-releasing cells in response to C9orf72 in healthy controls (HC; n = 28) and donors with ALS (n = 28). (**c**) Ratio of the number of cells releasing IFNγ and IL-5. Total (**d**), IFNγ- (**e**), IL-5- (**f**), and IL-10-mediated (**g**) T cell responses towards C9orf72 in ALS, HC, Parkinson's disease (PD; n = 15), and Alzheimer's disease (AD; n = 15) cohorts (ALS (n = 28) and HC (n = 28) are the same as in Fig. 2 and panels **a**–**c**). Proportion of IFNγ- (**h**) and IL-5-releasing (**i**) T cells among all cytokine-releasing cells, and ratio of the number of cells releasing IFNγ and IL-5 (**j**), in response to C9orf72 in HC, ALS, AD, and PD cohorts. P-values from two-tailed Mann–Whitney tests from comparisons of two groups, and from Kruskal-Wallis tests followed by Dunn's multiple comparisons test for comparison of four groups. Only significant p-values are shown, the complete list of p-values can be found in the Source Data file. Geometric mean ± 95% confidence interval is shown. Fold change (FC) values represent the ratio of geometric values in ALS/HC.

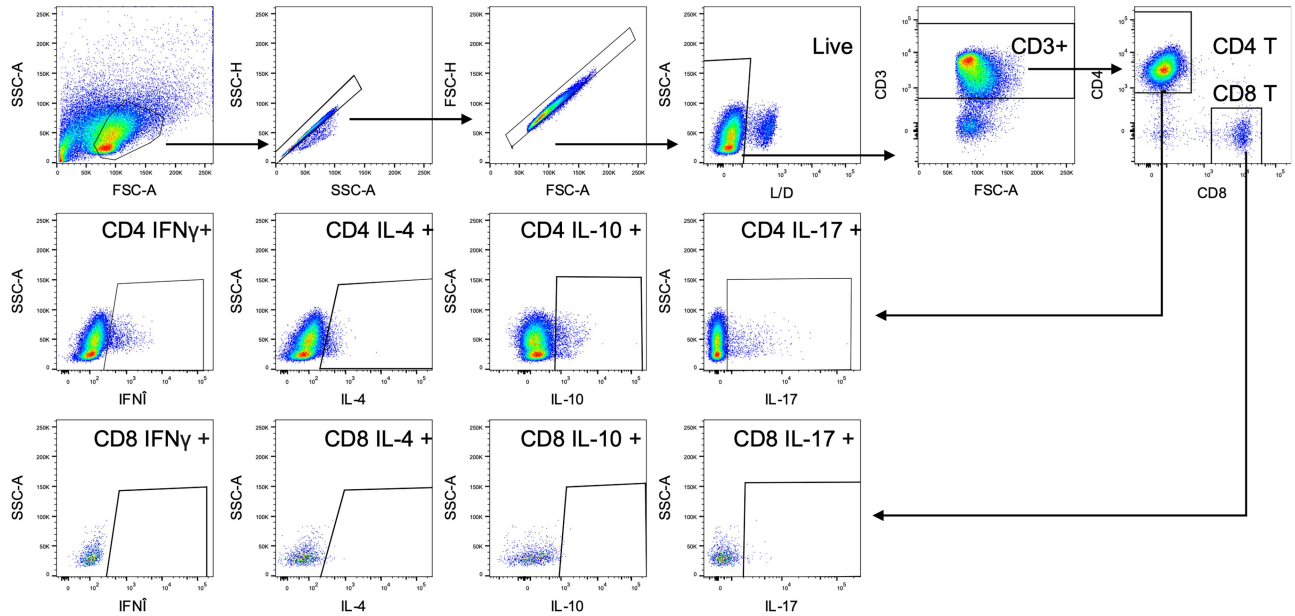

Extended Data Fig. 3 | Phenotyping of cytokine-secreting cells. Gating strategies for the identification of cytokine-expressing T cells 24 h post C9orf72 peptide pool restimulation of 2-week cell culture, in healthy controls (HC; $n = 30$) and donors with ALS ($n = 29$). Related to data in Fig. 4.

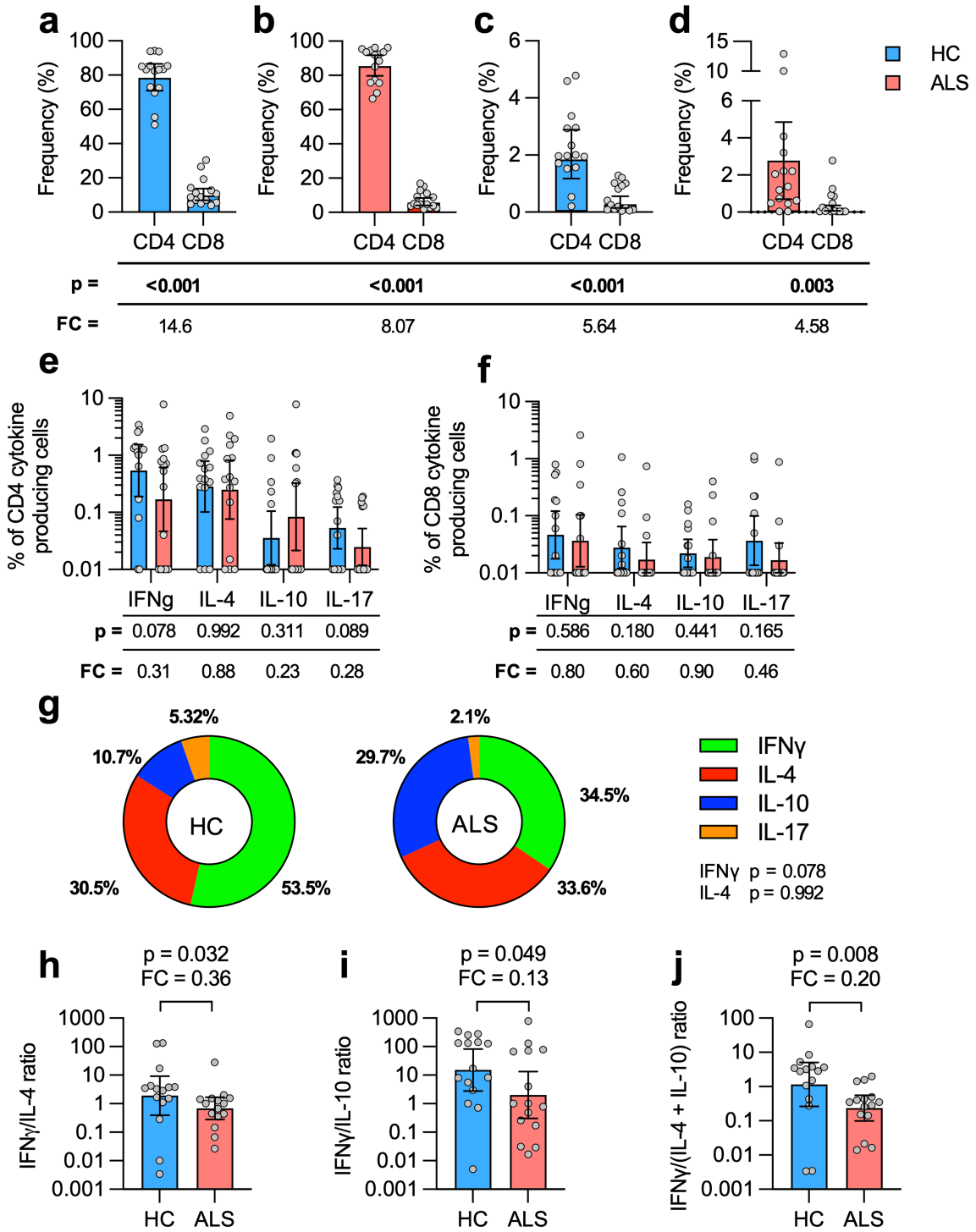

Extended Data Fig. 4 | Characterization of C9orf72-reactive T cells. Frequency of CD4 and CD8 T cells in HC (**a**) and ALS (**b**), as well as cytokine-expressing CD4 and CD8 T cells in HC individuals (n = 15) (**c**) and patients with ALS (n = 15) (**d**) 6 h post C9orf72 peptide pool restimulation of 2-week culture. Cytokine expression in CD4 (**e**) and CD8 (**f**) T cells in patients with ALS and HC individuals after C9orf72 peptide pool restimulation. (**g**) Overall sum of % CD4 and CD8 responses by the different cytokines. Ratios of the frequency of CD4 T cells expressing IFNγ and IL-4 (**h**), IFNγ and IL-10 (**i**), and IFNγ and cells expressing IL-4 or IL-10 (**j**). P-values are from two-tailed Mann–Whitney test, and geometric mean ± 95% confidence interval and fold change (FC) values are shown.

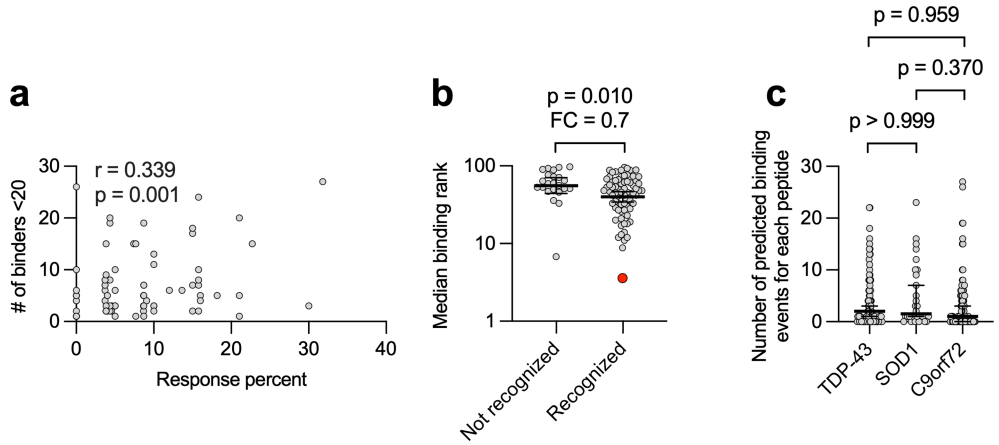

Extended Data Fig. 5 | Association between C9orf72 peptide immunogenicity and HLA binding. (**a**) Correlation between response frequency and number of predicted binding events for each peptide (n = 95) to the 27 most common HLA II allelic variants. Correlation is indicated by Spearman r and p-value. (**b**) Comparison of median binding rank to the 27 most common HLA II allelic variants for peptides recognized (n = 72) or not recognized (n = 23) in 28 patients with ALS. The most recognized peptide, aa56–DGEITFLANHTLNGE, is highlighted in red. P-value from two-tailed Mann–Whitney tests and geometric mean ± 95% confidence interval are shown. (**c**) Predicted binding events for each peptide from C9orf72, TDP-43, and SOD1, to the 27 most common HLA II allelic variants. P-values from two-tailed Kruskal-Wallis tests followed by Dunn's multiple comparison test, and median ± 95% confidence interval are shown.

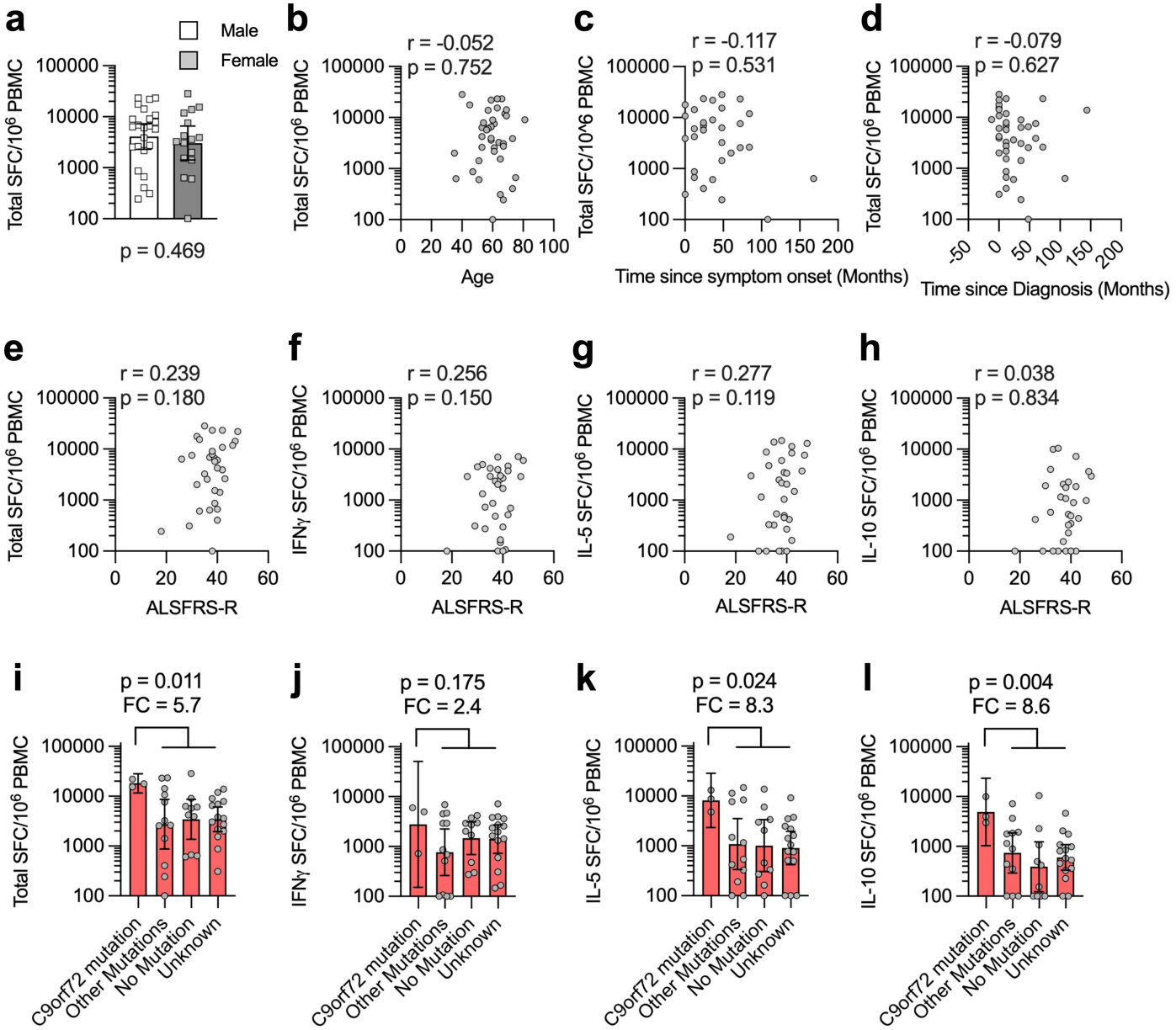

Extended Data Fig. 6 | Correlation between C9orf72 responsiveness and clinical and biological variables. (**a**) Difference in magnitude of response between ALS samples from male (n = 24) and female (n = 16) individuals. P-value from two-tailed Mann–Whitney tests and geometric mean ± 95% confidence interval are shown. Correlation between C9orf72 response and age (n = 40) (**b**), time since onset (n = 31) (**c**), and time since diagnosis (n = 40) (**d**) against the magnitude of C9orf72-specific reactivity. Correlation between ALSFRS-R score and Total (**e**), IFNγ- (**f**), IL-5- (**g**), and IL-10- (**h**) mediated C9orf72 responses in donors with ALS (n = 33). Correlation is indicated by Spearman r and p-value. Total (**i**), IFNγ- (**j**), IL-5- (**k**), and IL-10-mediated (**l**) T cell responses towards C9orf72 for participants with ALS carrying the C9orf72 mutation (n = 3), compared to the remaining participants with ALS, either carrying other mutations (ataxin-2, CHCHD10, FIG4, NEK1, SOD1, and TBK1) (n = 12), or carrying none of those mutations (n = 10), or those for which the genetic data were not available (unknown; n = 15). P-values from two-tailed Mann–Whitney tests and geometric mean ± 95% confidence interval are shown for histograms.

Extended Data Table 1 | Characteristics of the study cohorts

	HC (n=28)	ALS (n=40)	*p value*[a]
Sex (male/female)			
Male	19	24	
Female	9	16	p = 0.612
Age (median, range)			
Total	59.0 (Range 29-82)	61.0 (Range 45-81)	p = 0.680
Male	59.0 (Range 29-82)	61.0 (Range 45-81)	p = 0.441
Female	59.0 (Range 34-68)	59.0 (Range 35-68)	p = 0.770
Months since Symptom Onset (Median, Range, n[b])		36.0 (Range 0-168, n=31)	
Total			
Male		24.0 (Range 0-84, n=19)	
			p = 0.023
Female		48.0 (Range 0-168, n=12)	
Months since diagnosis Onset (Median, Range)		12.0 (Range -12-144)	
Total			
Male		12.0 (Range -12-72)	
			p = 0.599
Female		18.0 (Range 0-144)	
ALSFRS-R (Median, Range, n[b])		38.0 (Range 18-48, n=33)	
Total			
Male		39.0 (Range 18-48, n=20)	
			p = 0.438
Female		37.0 (Range 30-46, n=13)	

[a]Fisher's exact test comparing the number of male and female participants, Mann–Whitney test for comparing age, months since symptom onset, months since diagnosis and Revised ALS Functional Rating Scale (ALSFRS-R).

[b]Number (*n*) of donors for whom variable information was available. Information for remaining variable was available for all donors.

Extended Data Table 2 | Characteristics of the PD and AD cohorts

	PD (n=15)	AD (n=15)	*p value*[a]
Sex (male/female)			
Male	12	9	p = 0. 427
Female	3	6	
Age (median, range)			
Total	70.0 (Range 58-81)	74.0 (Range 56-87)	p = 0. 253
Male	71.5 (Range 58-81)	74.0 (Range 68-78)	p = 0. 334
Female	69.0 (Range 63-77)	72.0 (Range 56-87)	p = 0. 548
MoCA (median, range, n[b])			
Total	26.0 (Range 12-30, n=12)	18.0 (Range 10-24, n=9)	p = 0. 004
Male	26.0 (Range 12-30, n=9)	17.0 (Range 10-24, n=4)	p = 0. 053
Female	26.0 (Range 26-29, n=3)	19.0 (Range 16-24, n=5)	p = 0. 036
UPDRS III (median, range, n[b])			
Total	20.5 (Range 9-44, n=11)		
Male	22.0 (Range 9-44, n=9)		
Female	13.5 (Range 13-14, n=2)		

[a]Fisher's exact test comparing the number of male and female participants, Mann–Whitney test for comparing age.
[b]Number (*n*) of donors for whom variable information was available. Information for remaining variables was available for all donors. UPDRS (III): Unified Parkinson's Disease Rating Scale, part III. MoCA: Montreal Cognitive Assessment.

Extended Data Table 3 | Characteristics of the University of California, San Diego validation cohorts

	C9orf72 mutation carriers (n=7)	No mutation (n=7)	*p value*[a]
Sex (male/female)			
Male	3	4	p > 0.999
Female	4	3	
Age (median, range)			
Total	49.0 (Range 42-65)	54.0 (Range 42-82)	p = 0.330
Male	46.0 (Range 42-49)	54.0 (Range 42-54)	p = 0.229
Female	58.0 (Range 47-65)	79.0 (Range 64-82)	p = 0.114
Months since Symptom Onset (Median, Range)			
Total	24.0 (Range 0-48)	24.0 (Range 12-48)	p = 0.803
Male	36.0 (Range 12-48)	30.0 (Range 12-48)	p = 0.971
Female	18.0 (Range 0-36)	24.0 (Range 12-36)	p = 0.771
Months since diagnosis (Median, Range, n[b])			
Total	12.0 (Range 0-36)	12.0 (Range 0-36, n=6)	p = 0.469
Male	12.0 (Range 12-12)	12.0 (Range 12-36, n=3)	p > 0.999
Female	0.0 (Range 0-36)	12.0 (Range 0-24, n=3)	p = 0.657

[a]Fisher's exact test comparing the number of male and female participants, Mann–Whitney test for comparing age, months since symptom onset and months since diagnosis
[b]Number (*n*) of donors for whom variable information was available. Information for remaining variables was available for all donors.

nature portfolio

Corresponding author(s): David Sulzer

Last updated by author(s): Aug 6, 2025

Reporting Summary

Nature Portfolio wishes to improve the reproducibility of the work that we publish. This form provides structure for consistency and transparency in reporting. For further information on Nature Portfolio policies, see our Editorial Policies and the Editorial Policy Checklist.

Statistics

For all statistical analyses, confirm that the following items are present in the figure legend, table legend, main text, or Methods section.

n/a	Confirmed	
☐	☒	The exact sample size (*n*) for each experimental group/condition, given as a discrete number and unit of measurement
☐	☒	A statement on whether measurements were taken from distinct samples or whether the same sample was measured repeatedly
☐	☒	The statistical test(s) used AND whether they are one- or two-sided *Only common tests should be described solely by name; describe more complex techniques in the Methods section.*
☒	☐	A description of all covariates tested
☐	☒	A description of any assumptions or corrections, such as tests of normality and adjustment for multiple comparisons
☐	☒	A full description of the statistical parameters including central tendency (e.g. means) or other basic estimates (e.g. regression coefficient) AND variation (e.g. standard deviation) or associated estimates of uncertainty (e.g. confidence intervals)
☐	☒	For null hypothesis testing, the test statistic (e.g. *F*, *t*, *r*) with confidence intervals, effect sizes, degrees of freedom and *P* value noted *Give P values as exact values whenever suitable.*
☒	☐	For Bayesian analysis, information on the choice of priors and Markov chain Monte Carlo settings
☒	☐	For hierarchical and complex designs, identification of the appropriate level for tests and full reporting of outcomes
☒	☐	Estimates of effect sizes (e.g. Cohen's *d*, Pearson's *r*), indicating how they were calculated

Our web collection on statistics for biologists contains articles on many of the points above.

Software and code

Policy information about availability of computer code

Data collection	Flurospot data was aquired using the Mabtech IRIS system, with the Mabtech Apex (v2.0) software. Flow cytometry data from the Fortessa X-20 was acquired using the FACSDiva (v9.2) or using SpectroFlo flow cytometry software (Cytek, v3.3) for the Cytek Aurora.
Data analysis	Flow cytometry data was analyzed using FlowJo (v10.10.0). All statistical analyzes were performed using the GraphPad Prism (v10) software. No custom computer code or algorithm was used to generate results that are reported in the paper. Predicted peptide binding to HLA class II allelic variants were analyzed using the MHC-II Binding Prediction Results tool available at IEDB (http://tools.iedb.org/mhcii/), using the NetMHCIIpan 4.1 EL prediction method. HLA restrictions were inferred using the Restrictor Analysis Tool for Epitopes (RATE) hosted by the IEDB (http://tools.iedb.org/rate/). ALS donors were classified patients into one of five categories, with either a very short, short, intermediate, long, or very long predicted survival time, using the online ENCALS prediction model (http://tool.encalssurvivalmodel.org)

For manuscripts utilizing custom algorithms or software that are central to the research but not yet described in published literature, software must be made available to editors and reviewers. We strongly encourage code deposition in a community repository (e.g. GitHub). See the Nature Portfolio guidelines for submitting code & software for further information.

Data

Policy information about availability of data

All manuscripts must include a data availability statement. This statement should provide the following information, where applicable:

- Accession codes, unique identifiers, or web links for publicly available datasets
- A description of any restrictions on data availability
- For clinical datasets or third party data, please ensure that the statement adheres to our policy

Source data for all figures are provided with this paper. FCS files and FlowJo workspace files have been uploaded to Zenodo (Spectral files: https://doi.org/ 10.5281/zenodo.16749283, ICS files: https://doi.org/10.5281/zenodo.16749334, https://doi.org/10.5281/zenodo.16754553, https://doi.org/10.5281/zenodo.16754591, https://doi.org/ 10.5281/zenodo.16754609).

Research involving human participants, their data, or biological material

Policy information about studies with human participants or human data. See also policy information about sex, gender (identity/presentation), and sexual orientation and race, ethnicity and racism.

Reporting on sex and gender	During the study recruitment we recruited as many donors as possible, and therefore did not consider sex or gender. Reflecting a male bias in the risk of developing ALS and the higher number of males participating in the clinical site participating in the study, we have more male (24/40) than female (16/40) ALS study participants in this study. However, there was no significant difference compared to the healthy controls in regards to the proportion of male (19/28) and female (9/28) study participants. Importantly, we did not observe a difference in the T cell response to C9orf72 when comparing male and female ALS study participants. Sex and gender were self-reported by study participants. The ALS validation cohort of 7 C9orf72 mutation carriers and 7 sporadic ALS donors. The number of male and female donors was very similar between the two groups, with the C9orf72 carrier group consisting of 3 male and 4 female donors, and the sporadic ALS group consisting of 4 male and 3 female donors. Similar to the ALS and healthy control cohorts, there were more male participants among the PD (12/15) and AD (9/15) than female participants.
Reporting on race, ethnicity, or other socially relevant groupings	During the study recruitment we recruited as many donors as possible, and therefore did not consider race or ethnicity. No racial, ethnical, or socially relevant categorization information was collected during participant recruitment.
Population characteristics	In the present study we included ALS and healthy control (HC) study participants of very similar age range, ALS median 61.0 years (range 45-81) and HC median 59.0 years (range 29-82). As described above, the frequency of male and female participants similar between the ALS and HC cohorts. Genetic information regarding mutations known to confer risk of developing ALS was tested in 26/40 ALS participant. For all ALS participants time since diagnosis was recorded, for 36/40 participants time since symptom onset was recorded, and for 33/40 participants the Revised Amyotrophic Lateral Sclerosis Functional Rating Scale was recorded. We further included samples from 14 ALS donors as part of a validation cohort, consisting of 7 carriers of the C9orf72 mutation and 7 sporadic ALS donors. These donors were of very similar age, median 49.0 (range 42-65) and 54.0 (range 42-82) for the C9orf72 mutation carriers and sporadic ALS donors, respectively. The median age of PD and AD donors were 70 (range 58-81) and 74 (range 56-87), respectively.
Recruitment	This study used samples from donors recruited by several physician collaborators in their ALS/Neuro clinics around the United States: Emory University (Atlanta, Georgia), the National Institute for Neurological Disorders and Stroke at the National Institute of Health (Bethesda, Maryland), the University of California, Irvine (Irvine, California), University of California San Diego (San Diego, California), and Harvard Medical School/Massachusetts General Hospital (Boston, Massachusetts). In addition, donors were recruited and samples obtained from a Contract Research Organization, Sanguine Biosciences. Inclusion criteria for ALS donors included i) ALS subjects diagnosed with familial/sporadic ALS according to the El Escorial criteria, ii) subjects must be 20 years of age or older at the time of symptom onset, and iii) the ability to provide informed consent. Exclusion criteria included i) other major neurological or medical diseases that could cause progressive weakness or cognitive dysfunction, and ii) an unstable medical condition that would make participation unsafe. Inclusion criteria for age/sex-matched HC included i) age including 53-82, ii) sex, and iii) the ability to provide informed consent. Exclusion criteria for HC were the same as ALS except for the addition of self-reported ALS genetic risk factors (i.e., ALS in first-degree blood relatives). ALS diagnosis was based on clinical criteria, i.e., a person's symptoms and examination findings. Typically, the diagnosis was associated with clinical findings of upper and lower motor dysfunction and a progressive course and failure of diagnostic tests such as brain and spinal cord MRI, electrophysiological testing, and routine laboratory studies to identify an alternative cause. If the clinical presentation deviates from these typical features, a neuromuscular specialist with extensive experience in diagnosing ALS was consulted to adjudicate the diagnosis. Subjects with PD (n=15) were recruited by the Movement Disorders Clinic at the Department of Neurology at CUMC. Inclusion criteria for the patients consisted of i) clinically diagnosed PD with the presence of bradykinesia and either resting tremor or rigidity, ii) PD diagnosis between ages 35–80, iii) history establishing dopaminergic medication benefit, and iv) ability to provide informed consent. Exclusion criteria for PD were i) atypical parkinsonism or other neurological disorders, ii) history of cancer within past 3 years, iii) autoimmune disease, and iv) chronic immune modulatory therapy. The recruited individuals with PD all met the UK Parkinson's Disease Society Brain Bank criteria for PD.

Subjects with AD (n=15) were recruited from the Alzheimer's Disease Research Center at CUMC or from PrecisionMed (a fee-for-service, contract research organization). Subjects recruited from CUMC were diagnosed by neurologists according to the National Institute of Aging and Alzheimer's Association criteria; AD subjects recruited from PrecisionMed were diagnosed according to NINCDS-ADRDA criteria, by a neurologist or internist. The AD and PD donors were selected to be age- and sex-matched to the ALS donors.

Ethics oversight

All participants provided written informed consent for participation in the study. Ethical approval was obtained from the Institutional Review Boards at La Jolla Institute for Immunology (LJI; Protocol number: VD-124, VD-118, VD-155, and VD-171), Massachusetts General Hospital (MGH; Protocol number: 2006P000982), Emory (Protocol number: CR003-IRB00078771), University of California Irvine (UCI, Protocol number: 20163191), National Institutes of Health (NIH, Protocol number: 17N0131), University of California San Diego (UCSD, Protocol number: 120295), and Columbia University Irving Medical Center (CUMC, Protocol number IRB-AAAQ9714 and AAAS1669). Research activities conducted with samples from Sanguine Biosciences or PrecisionMed (fee-for-service, contract research organizations) are not considered human subjects research under Health and Human Services (HHS) regulations.

Note that full information on the approval of the study protocol must also be provided in the manuscript.

Field-specific reporting

Please select the one below that is the best fit for your research. If you are not sure, read the appropriate sections before making your selection.

☒ Life sciences ☐ Behavioural & social sciences ☐ Ecological, evolutionary & environmental sciences

For a reference copy of the document with all sections, see nature.com/documents/nr-reporting-summary-flat.pdf

Life sciences study design

All studies must disclose on these points even when the disclosure is negative.

Sample size	As this is a descriptive observational study, no sample size calculation was performed. As many participants as possible were used for the experiment.
Data exclusions	No data was excluded from analysis.
Replication	All conditions were tested in triplicate for the flurospot assay. Responses were considered positive if they met all three criteria: i) DMSO background subtracted spot forming cells per 10^6 were ≥ 100, ii) stimulation index ≥ 2 compared to DMSO controls, and iii) p≤ 0.05 by Student's t-test or Poisson distribution test. The positive flurospot responses towards C9orf72 was confirmed for all ALS donors included in the deconvolution of T cell responses towards individual peptides. The spectral flow cytometry immunophenotyping were performed once for each of the 20 healthy control and 19 ASL participants. Flow cytometry analyses of cytokine releasing cells in response to C9orf72 peptide pool was performed once for each of the 28 healthy control and 28 ALS participants.
Randomization	The same number of ALS and healthy control (HC) samples were included in each experiment, to reduce the risk of technical biases. The ALS and HC donors were randomly assigned to the individual experiment. Donors were randomly allocated to experimental groups.
Blinding	We were not blinded with regards to the disease status of each study participants to ensure that we could include the same number of ALS and healthy control samples per experiment. All Fluorospot data was acquired by an automated process, which eliminates the introduction of bias.

Reporting for specific materials, systems and methods

We require information from authors about some types of materials, experimental systems and methods used in many studies. Here, indicate whether each material, system or method listed is relevant to your study. If you are not sure if a list item applies to your research, read the appropriate section before selecting a response.

Materials & experimental systems

n/a	Involved in the study
☐	☒ Antibodies
☒	☐ Eukaryotic cell lines
☒	☐ Palaeontology and archaeology
☒	☐ Animals and other organisms
☒	☐ Clinical data
☒	☐ Dual use research of concern
☒	☐ Plants

Methods

n/a	Involved in the study
☒	☐ ChIP-seq
☐	☒ Flow cytometry
☒	☐ MRI-based neuroimaging

Antibodies

Antibodies used

Antibodies flow cytometry
Cytek Aurora
CD4, APC-eF780, Clone: RPA-T4, 47-0049-42, ThermoFisher
CD8, BUV496, Clone: RPA-T8, 612942, BD
CD56, APC, Clone: 5.1H11, 362504, Biolegend
gdTCR, BV421, Clone: 11F2, 744870, BD
CCR4, PE Cy-7, Clone: G1, 557864, BD
CD14, BV480, Clone: M5E2, 746304, BD
CD161, BV650, Clone: DX12, 563864, BD
CXCR3, PE, Clone: G025H7, 353706, Biolegend
CD19, BV605, Clone: HIB19, 302244, Biolegend
CD3, BUV805, Clone: UCHT1, 612895, BD
CCR7, BV785 Clone: G043H7, 353216, Biolegend
CCR6, BUV395, Clone: 11A, 743356, BD
CD26, FITC, Clone: BA5b, 302704, Biolegend
CD45, PE Dazzle594, Clone: HI30, 982308, Biolegend
CD45RA, BV570, Clone: HI100, 304132, Biolegend
L/D, eFluor 506, 65-0866-14, ThermoFisher

Fortessa X-20
L/D, eFluor 506, 65-0866-14, ThermoFisher
CD4, APC-eF780, Clone: RPA-T4, 47-0049-42, ThermoFisher
CD3, AF700, Clone: UCHT1, 56-0038-42, ThermoFisher
CD8, BV650, Clone: RPA-T8, 301042, Biolegend
IL-10, APC, Clone: JES3-19F1, 506807, Biolegend
IL-4, BV421, Clone: MD425D2, 500826, Biolegend
IFNγ, FITC, Clone: 4S.B2, 11-7319-82, ThermoFisher
IL-17, BV785, Clone: BL168, 512338, Biolegend

Mabtech antibodies (From FluoroSpot Plus: Human IFN?γ/IL?10/IL?5 kit, cat nr FSP-010708-10)
human IFNγ, clone: 1-D1K
mouse anti-human IL-5, clone: TRFK5
mouse anti-human IL-10, clone: 9D7
mouse anti-human IFNγ BAM, clone: 7-B6-1-FS-BAM
mouse anti-human IL-5 WASP, clone: 5A10-WASP
mouse anti-human L-10 biotin, clone: 12G8-biotin
anti-BAM-490
anti-WASP-640
Streptavidin-550

Validation

Each reagent was handled as per manufacturer's instructions, however, the concentration of each antibody was determined by titration prior to the assay, to obtain the best signal-to-noise ratio. The dilution used for each antibody is shown in Supplementary Table S2

Plants

Seed stocks

N/A

Novel plant genotypes

N/A

Authentication

N/A

Flow Cytometry

Plots

Confirm that:

☒ The axis labels state the marker and fluorochrome used (e.g. CD4-FITC).

☒ The axis scales are clearly visible. Include numbers along axes only for bottom left plot of group (a 'group' is an analysis of identical markers).

☒ All plots are contour plots with outliers or pseudocolor plots.

☒ A numerical value for number of cells or percentage (with statistics) is provided.

Methodology

Sample preparation	Venous blood was collected from each participant in either heparin or EDTA-containing blood bags or tubes, as previously reported and described. PBMCs were isolated from whole blood by density gradient centrifugation using Ficoll-Paque Plus (GE #17144003). In brief, blood was first spun at 1850 rpm for 15 mins with brakes off to remove plasma. Plasma-depleted blood was then diluted with RPMI, and 35 mL of blood was carefully layered on tubes containing 15 mL Ficoll-Paque plus. These tubes were centrifuged at 1850 rpm for 25 mins with the brakes off. The interphase cell layer resulting from this spin was collected, washed with RPMI, counted, and cryopreserved in 90% v/v FBS and 10% v/v dimethyl sulfoxide (DMSO), and stored in liquid nitrogen until tested. The detailed protocol for PBMC isolation can be found at protocols.io (https://dx.doi.org/10.17504/protocols.io.bw2ipgce).
Instrument	Fluorospot data was acquired using the Mabtech IRIS system (Mabtech), flow cytometry data using the Fortessa X-20 (BD Biosciences) or the Cytek Aurora (Cytek Biosciences).
Software	Fluorospot data was acquired using the Mabtech IRIS system, with the Mabtech Apex (v2.0) software. Flow cytometry data from the Fortessa X-20 was acquired using the FACSDiva (v9.2) or using SpectroFlo flow cytometry software (Cytek, v3.3) for the Cytek Aurora.
Cell population abundance	No sorting was performed.
Gating strategy	The gating strategy is provided in Supplemental Figure S1, including the starting gates. For the Spectral flow cytometry panel, cells of interest was first identified using the FSC-H vs Time gate, followed by FSC-A x SSC-A to identify lymphocytes and monocytes, then FSC-H x FSC-A and SSC-H x SSC-A to identify single cells, followed by exclusion of non-viable (viability dye positive) and non-hematopoietic (CD45-) cells. For the intracellular cytokine staining panel, T cells were identified using the by FSC-A x SSC-A to identify lymphocytes, then FSC-H x FSC-A and SSC-H x SSC-A to identify single cells, followed by exclusion of non-viable (viability dye positive), and finally identification of CD3+ T cells.

☒ Tick this box to confirm that a figure exemplifying the gating strategy is provided in the Supplementary Information.